*sustainability*

MDPI

*Review*

# Study and Application Status of Ultrasound in Organic Wastewater Treatment

**Nannan Wang [1,*], Liangwei Li [1], Kai Wang [2], Xitong Huang [1], Yanhe Han [1], Xuejiao Ma [1], Menghan Wang [1], Xiao Lv [1] and Xinming Bai [1,*]**

[1] Department of Environmental Engineering, Beijing Institute of Petrochemical Technology, Beijing 102617, China; 2021520045@bipt.edu.cn (L.L.); 2022310432@bipt.edu.cn (X.H.); hanyanhe@bipt.edu.cn (Y.H.); maxuejiao@bipt.edu.cn (X.M.); 2021310613@bipt.edu.cn (M.W.); 2021310560@bipt.edu.cn (X.L.)

[2] Department of Energy Engineering, Beijing Institute of Petrochemical Technology, Beijing 102617, China; 0020160002@bipt.edu.cn

* Correspondence: wnn_flying@163.com (N.W.); 2022310441@bipt.edu.cn (X.B.)

**Abstract:** Ultrasound waves have been widely used in the field of organic wastewater treatment due to their mechanical, thermal, and chemical effects derived from their cavitation effect. Many researchers have combined ultrasound waves with other organic wastewater treatment methods because they have the potential to offset the disadvantages of other methods. In recent years, many authors within the literature have reviewed the application of ultrasound combined with a certain wastewater treatment method. In this review, we introduce the working mechanism of ultrasound in the treatment of organic wastewater and then examine the synergistic effects of ultrasound with other organic wastewater treatment methods based on various applications, indicating a strong synergistic effect between ultrasound and other wastewater treatment methods. Subsequently, we introduce typical ultrasound-enhanced organic wastewater treatment equipment and propose some possible developmental directions for ultrasound in the treatment of organic wastewater.

**Keywords:** cavitation mechanism; ultrasound operation mode; ultrasound reactor; organic wastewater treatment; physical fields

check for updates

**Citation:** Wang, N.; Li, L.; Wang, K.; Huang, X.; Han, Y.; Ma, X.; Wang, M.; Lv, X.; Bai, X. Study and Application Status of Ultrasound in Organic Wastewater Treatment. *Sustainability* **2023**, *15*, 15524. https://doi.org/10.3390/su152115524

Academic Editor: Agostina Chiavola

Received: 14 September 2023
Revised: 27 October 2023
Accepted: 31 October 2023
Published: 1 November 2023

**Copyright:** © 2023 by the authors. Licensee MDPI, Basel, Switzerland. This article is an open access article distributed under the terms and conditions of the Creative Commons Attribution (CC BY) license (https://creativecommons.org/licenses/by/4.0/).

## 1. Introduction

With the rapid development of industry in recent decades, environmental pollution has become a concern worldwide, because it seriously hinders the sustainable development of our world [1]. Organic wastewater is one of the main pollution sources because of toxic refractory organic pollutants in wastewater, which can be enriched in the human body and animals through the food chain; this seriously endangers human health and natural ecology [2]. The main types of organic wastewater include dye wastewater, pharmaceutical wastewater, coking wastewater, atrazine wastewater, high saline petrochemical wastewater, dairy wastewater, etc. [3–12]. In order to effectively eliminate organic pollutants in wastewater, many methods have been explored, and they can be divided into a chemical oxidation degradation process [13], biochemical degradation process [14], and physicochemical degradation process. However, every method has shortcomings [15]. Against this backdrop, some physical fields such as an ultrasound field, MW field, and UV/visible light field were introduced to compensate for these shortcomings, thus enhancing the treatment efficiency of wastewater.

In these physical fields, the ultrasound field is different from other physical fields because it belongs to a mechanical field, while other physical fields belong to the electromagnetic field; ultrasound works by relying on high-frequency vibrations and a subsequent cavitation effect [16]. According to the definition from the American National Standards Institute, ultrasound is a type of dense longitudinal wave with a frequency of >20 kHz; it can

be generated by a piezoelectric effect (generated by the interaction of mechanical pressure and electricity) or magnetostriction (generated in electromagnetic fields) [17]. Ultrasound can transmit strong energy and produce a considerable impact between interfaces when it is propagated in a gas, liquid, or solid, accompanied with the consumption of energy and the corrosion of equipment and materials [18,19]. As the application of ultrasound in the treatment of organic wastewater does not involve the addition of chemicals and does not cause secondary pollution [20], ultrasound is welcomed by many researchers, and it has been applied in combination with other treatment methods such as electrochemistry oxidation, photocatalytic oxidation, FE oxidation, membrane filtration, and PS oxidation [21]; its excellent enhancement capacity to various treatment methods of organic wastewater has been confirmed by many reports [22–24].

Recently, there have been several reviews on the combination of ultrasound with other wastewater treatment methods [25]. Hassani et al. [26] summarized the mechanism of ultrasound, reactor strategy, and basic principles of wastewater treatment. Yang et al. [24] summarized the factors that influence the treatment efficiency of wastewater in a combination of ultrasound with PS, as well as the degradation path of organic pollutants. Andrade et al. [27] used pollutants as classification indicators and introduced the degradation of persistent organic pollutants in the ultrasound field. However, a more comprehensive and systematic review of ultrasound, including the working mechanism, the work mode, the application in organic wastewater treatment, and the classification of ultrasound reactors, has not been published until now. In this review, we introduce the working mechanism of ultrasound, followed by its working mode, including working alone and coupling with other physical fields and organic wastewater treatment methods. Subsequently, we introduce typical ultrasound-enhanced organic wastewater treatment reactors. Finally, we propose possible research directions of ultrasound in the treatment of organic wastewater. Our review will promote the understanding of ultrasound in the treatment of organic wastewater.

## 2. Cavitation Mechanism of Ultrasound in the Treatment of Organic Wastewater

The cavitation effect of ultrasound in the liquid medium is the basis of many applications of ultrasound [28]. As shown in Figure 1, the propagation of ultrasound in the liquid medium can cause the compression and expansion of the solution to form local negative pressure. When the local negative pressure exceeds the tensile strength of water, cavities (the precursor of cavitation bubble) will be formed. Subsequently, ultrasound can form an oscillating sound (pressure) field on the formed cavities, causing a pressure cycle (high pressure compresses the gas in the bubble, and low pressure makes the gas expand) to promote the growth of bubbles. When the size of the bubble reaches a resonance radius, it is strongly coupled with the acoustic field and grows to the maximum value. Finally, the bubble breaks down and decomposes into small bubbles, which dissolve or continue to participate in the cavitation process [29]. The violent collapse of a cavitation bubble can generate shock waves, micro jets, ·OH, and high pressure, which can further produce mechanical, chemical, and thermal effects.

Research has shown that the wider the range of ultrasound cavitation, the greater the intensity, the stronger the activity of ultrasound chemical reactions, and the more significant the effect of ultrasound cavitation. However, the cavitation effect of ultrasound alone is not significant, and many researchers are committed to improving the cavitation effect of ultrasound, including adding solid particles and mechanical stirring in the system. Researchers usually add solid particles to the system or introduce mechanical stirring to enhance cavitation. Ultrasound cavitation is expressed by Equations (1) and (2) [30]:

$$\tau = 0.915 R_m \left( \frac{\rho}{P_m} \right)^{\frac{1}{2}} \left( 1 + \frac{P_{vg}}{P_m} \right) \quad (1)$$

$$R_m = (1 \times 10^{-3}) \frac{4}{3\omega_\alpha} (P_A - P_h) \left( \frac{2}{\rho P_A} \right)^{\frac{1}{2}} [1 + \frac{2}{3P_h} (P_A - P_h)]^{\frac{1}{3}} \quad (2)$$

where $\tau$ is the collapse time of the cavitation bubble (ms); $R_m$ indicates the maximum bubble size ($\mu$m); $\rho$ is the density of the liquid (kg $m^{-3}$); $P_m$ is the pressure in the liquid (atm); $P_{vg}$ is the vapor pressure in the bubble (atm); $\omega_a$ denotes the ultrasound frequency (kHz); $P_A$ is the acoustic amplitude (dB); and $P_h$ is the hydrostatic pressure (atm).

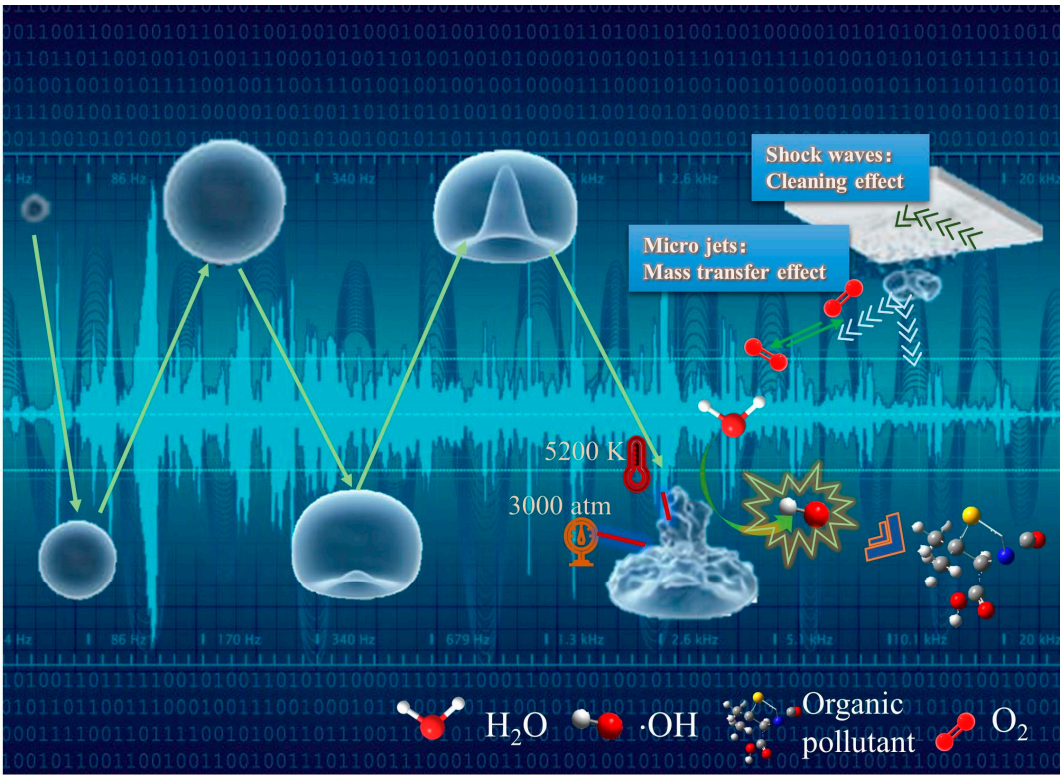



**Figure 1.** Mechanism diagram of ultrasound cavitation and degradation process of organic pollutants.

It can be seen from Equations (1) to (2) that ultrasound frequency ($\omega_a$) is inversely proportional to the maximum bubble size ($R_m$) and the collapse time of cavitation bubbles ($\tau$). Thus, an increase in ultrasound frequency ($\omega_a$) can increase the rate of cavitation via reducing the collapse time of cavitation bubbles ($\tau$) [4]. Nonetheless, an excessive increase in frequency may cause undesirable cavitation, i.e., the time of the rarefaction/compression cycle is shortened and the resonance radius of the bubble is reduced, meaning that the bubbles cannot grow to their optimal size [31,32], which leads to a decrease in the treatment efficiency of organic wastewater. In addition, an increase in frequency will lead to an increase in the cavitation threshold, hinder bubble nucleation, weaken the cavitation effect, and reduce the treatment efficiency of organic wastewater. Therefore, it is necessary to choose an appropriate frequency during the experimental process.

### *2.1. Mechanical Effect*

The cavitation effect of ultrasound can further lead to a mechanism effect by the generation of micro jets (300 m $s^{-1}$) and shock waves near the solid surface and in the solution, respectively [33] (Figure 1). The micro jets near the solid surface can refresh the solid surface, expose the reaction center, and increase the active surface area of functional materials by means of the pitting effect [33–35], while the shock waves in the solution can increase the mass transfer effect by increasing the liquid vibration. Micro jets and shock waves are always used to reduce the thickness of the diffusion layer on the surface of the electrode and increase the transmission of $O_2$ in the solution, respectively [36]. Furthermore,

the small droplets formed by the mechanical effect of ultrasound can make hydrophobic substances in water distribute uniformly, thus minimizing reagent dosage and reducing costs. Li et al. [3] used this process to electrolyze cationic red X-GRL and found that the mechanism effect of ultrasound can increase the removal rate of TOC from 56.0 to 67.6%.

### *2.2. Chemical Effect*

The chemical effect of ultrasound is supported by the generation of highly reactive radicals such as ·OH ($E^0$ = 2.8 V) and ·H in the liquid, which can directly oxidize organic wastewater (Figure 1). This effect is more significant when ultrasound frequency is higher than 100 kHz [33]. The chemical effect of ultrasound in the solution can be concluded by Equations (3)–(6).

$$H_2O \overset{(((}{\rightarrow} \cdot H + \cdot OH \quad (3)$$

$$O_2 \rightarrow 2O \quad (4)$$

$$O + H_2O \rightarrow 2 \cdot OH \quad (5)$$

$$\cdot H + O_2 \rightarrow \cdot OH + O \quad (6)$$

where ((( represents the ultrasound wave.

The degradation of organic pollutants in the ultrasound field can be divided into three types: (1) the degradation of hydrophilic pollutants in the bulk solution by the ·OH in the bulk solution, (2) the accumulation and degradation of hydrophobic non-volatile compounds via ·OH attacks and thermal reactions in the interfacial zone of cavitation bubbles, and (3) the pyrolysis of the volatile substances inside the cavitation bubbles [20].

What we should notice is that the content of ·OH in the interfacial zone is always higher than that in bulk solution, resulting in easier oxidation degradation for hydrophobic pollutants than that of hydrophilic pollutants. In the study of Serna-Galvis et al. [37], penicillin, which is a hydrophilic chemical, could not be incompletely mineralized (removal rate of TOC = 99.0%) by ·OH. Conversely, perfluorooctanoic acid, which is a non-volatile substance, could be completely degraded at the gas–liquid interface [38].

### *2.3. Thermal Effect*

The shock waves generated by the violent collapse of a cavitation bubble can strongly squeeze surrounding water molecules, followed by the generation of high pressure ($1.8 \times 10^3$–$3 \times 10^3$ atm), which can further produce local high temperature ($5.2 \times 10^3$ K) by transferring energy to water molecules [33] (Figure 1). High temperature can lead to the pyrolysis of chemical bonds in chemical compounds and thus promote the degradation of organics in wastewater [35]. Two typical applications of the thermal effect of ultrasound are to activate PS by breaking the O-O bond to produce sulphate radical ($SO_4^{-\cdot}$) and decompose the nearby water molecules to generate ·OH. In addition, the thermal effect of ultrasound can promote mass transfer by improving the molecular thermal movement [33].

## 3. Working Mode of Ultrasound in the Treatment of Organic Wastewater

### *3.1. Work Alone*

Ultrasound alone can be used in the treatment of organic wastewater, relying on the chemical effects for a low-frequency vibration and the mechanical effect for a high-frequency vibration. In the working atmosphere of low-frequency vibration, ultrasound can directly degrade organic pollutants and weaken the toxicity of wastewater by the generated ·OH; this has been confirmed by the study of Cardenas Sierra et al. [20], in which a 40 kHz ultrasound separately oxidized cephalosporin toxin and doxycycline in two antibiotic wastewaters, and the toxicity of the treated antibiotic wastewaters was decreased by 36.0% and 87.0%, respectively, whereas the removal rate of cephalosporin toxin and doxy-

cycline sharply decreased to 1.6% and 3.8%, respectively, in the presence of isopropanol as ·OH scavenger.

As for high-frequency ultrasound, it is seldom applied in the common treatment process of organic wastewater but rather in the treatment of special wastewater such as oil shale retorting wastewater. As the high-frequency vibration of ultrasound can throw away the water molecules on the surface of water into the air to form mist, Matouq et al. [39] applied high-frequency ultrasound with a frequency of 1700 kHz to treat oil shale retorting wastewater in order to separate water, and dissolved organic compounds by means of evaporation and condensation. The conductivity of the condensate declined remarkably with the residue, revealing the successful separation of water, and dissolved organic compounds.

Besides the direct treatment of organic wastewater, low-frequency ultrasound can indirectly remove N and P from wastewater by improving the permeability of the cell membrane of algal that can adsorb N and P as nutrients. With the improvement in the permeability of the cell membrane, N and P can easily penetrate the cell membrane and be absorbed by algae, thus promoting the removal of N and P from organic wastewater. Ren et al. [40] found that the removal rates of TN and TP in organic wastewater had a remarkable increase after the introduction of ultrasound; the removal rates of TN and TP were >96.0% and >97.0%, respectively.

Although ultrasound alone can effectively treat organic wastewater, high energy consumption has always been the primary limitation of the usage of ultrasound alone. Thus, most researchers have focused their attention on combining ultrasound with other methods to simultaneously obtain a high treatment efficiency of organic wastewater and a low consumption of energy.

### *3.2. Combination with Other Physical Fields*

#### 3.2.1. Combination of Ultrasound Field with EC Process

As we have previously mentioned, the synergistic effect of ultrasound with the EC processes is attributed to the mechanical effect of ultrasound. The remarkable effect of ultrasound can be verified by observing the particle state before and after the reaction with SEM. After reaction, the particle size of the filler and the surface roughness significantly increase, many fine holes are produced, and the local microspores collapse, which increases the specific surface area of the micro-electrolytic filler and enhances the ability to absorb pollutants in wastewater in the presence of ultrasound. Table 1 summarizes some typical applications of the ultrasound-assisted EC process in the treatment of organic wastewater. Chang et al. [41] reported that ultrasound treatment can improve the removal rate of Cu from 55.7 to 95.6% and decompose EDTA (removal rate of COD = 84.0%, Table 1; No. 12). The degradation rate constant after ultrasound treatment is 100 times that without ultrasound treatment [41]. In this system, ultrasound frequency is a key factor affecting the removal rate of pollutants. An increase in ultrasound frequency will increase the number of cavitation bubble that collapse, thereby increasing the cavitation effect and the production of ·OH. When the frequency is too high, the energy in the solution will be rapidly consumed, resulting in the same chemical effect that requires more energy, and ·OH is easily bound to water before the cavitation bubble ruptures.

During this process, the range of ultrasound frequency is approximately 20–45 kHz as excessive frequency can lead to the recombination of ·OH with ·OH or with ·H [34]. Within this range, the mass transfer effect generated by the ultrasound mechanical effect is the main influence. However, Yousefi et al. [32] achieved a better removal efficiency at a high frequency of 130 kHz when using this process to degrade high saline petrochemical wastewater. Although some ·OH recombines within this range, the lifespan of cavitation bubbles decreases and the cavitation effect is significantly enhanced, which can better diffuse ·OH into the solution and increase the removal effect.

**Table 1.** Typical applications of ultrasound-assisted EC process in organic wastewater treatment.

| No. | Study System | Pollutants | Ultrasound | | Experimental Conditions | Removal Efficiency | Ref. |
|---|---|---|---|---|---|---|---|
| | | | Power (W) | Frequency (kHz) | | | |
| 1 | Ultrasound–EC | MB | 300 | - | reaction time = 60 min, V = 20 V, $Na_2SO_4$ = 15 g $L^{-1}$ | 94.9% | [31] |
| 2 | | Blue 49 | 150 | 35 | pH = 8.3, reaction time = 80.6 min, V = 0.7 V, dye = 10 mg $L^{-1}$ | COD = 90.1% | [42] |
| 3 | | Cephalosporin pharmaceutical | - | 45 | reaction time = 30 min, current of density = 8 mA $cm^{-2}$ | COD = 94.0% | [4] |
| 4 | | 2,4-dichlorophenoxyacetic acid | 200 | 24 | pH = 4.0, power consumption = 302.3 kWh $m^{-3}$, flow rate = 1 × $10^{-3}$ $dm^3$ $min^{-1}$, NaCl = 3 g $L^{-1}$ | - | [43] |
| 5 | Ultrasound–EC–chloride media | Methyl paraben | - | 20 | pH = 3.0, V = 2.8 V, methyl paraben = 100 mg $dm^{-3}$, $Na_2SO_4$ = 3 g $cm^{-3}$ | TOC = 100% | [44] |
| 6 | Ultrasound–EC–$MnSO_4/Na_2S_2O_8$ | Black 5 | 44 | - | pH = 8.05, V = 8 V, $Na_2SO_4$ = 100 mg $L^{-1}$, $MnSO_4$ = 75 mg $L^{-1}$ | TOC = 90.0% | [45] |
| 7 | Ultrasound–EC–PS | High saline petrochemical wastewater | 300 | 130 | pH = 3.0, reaction time = 120 min, PS = 20 mmol $L^{-1}$ | COD = 91.2% | [32] |
| 8 | Ultrasound–EC–FE | 2,4-dinitrotoluene, 2,4,6-trinitrotoluene | 20 | 28 | pH = 3.0, $Fe^{3+}$ = 0.1 mmol $L^{-1}$, 2,4-D = 1 mmol $L^{-1}$, DNOC = 0.5 mmol $L^{-1}$, AB = 0.025 mmol $L^{-1}$, $Na_2SO_4$ = 0.05 mol $L^{-1}$ | 100% | [34] |
| 9 | | Red X-GRL | 160 | 20 | pH = 3,0, $Fe^{2+}$ = 5 mmol $L^{-1}$, $Na_2SO_4$ = 0.05 mol $L^{-1}$, $H_2SO_4$ = 1 mol $L^{-1}$, NaOH = 1 mmol $L^{-1}$, T = 30 °C | 56.2% | [3] |
| 10 | | Textile wastewater | 350 | 40 | pH = 5.0, reaction time = 90 min, V = 0.5 V, COD = 1.25 × $10^3$ mg $L^{-1}$, electrolyte = 6 g $L^{-1}$, PS = 0.5 mmol $L^{-1}$ | COD = 96.0% | [46] |
| 11 | Ultrasound–micro electrolysis | Phenol | 300 | 28 | pH = 4.0, V = 3 V, iron dosage = 50 g $L^{-1}$, iron: carbon = 1:1, phenol = 100 mg $L^{-1}$ | 88.6% | [47] |
| 12 | Ultrasound–electrodeposition | EDTA-Cu | 157–300 | 20 | pH = 7.0, reaction time = 220 min, voltage gradient = 1.0 V $cm^{-1}$ | 84.0% | [41] |

3.2.2. Combination of Ultrasound Field with Photocatalytic Oxidation Process

It has been confirmed that light such as visible light (λ = 400–800 nm) and UV (λ = 200–400 nm) can produce electron–hole pairs by providing photons to photocatalyst, such as $TiO_2$ with energy equal to or greater than the band gap (Equation (7)), resulting in the photoexcitation of electrons from the filled valence band to the empty conduction band [48,49]. Like the photochemical process, ultrasound can excite electron–hole pairs as well rely on the light from sonoluminescence phenomenon generated by the collapse of a cavitation bubble (Equation (8)). Electron–hole pairs can further generate $HO_2\cdot$ and ·OH by reacting with $O_2$ and $H_2O$ (Equations (9)–(11)).

$$TiO_2 \overset{\text{visible light}}{\rightarrow} TiO_2\left(e^- + h^+\right) \quad (7)$$

$$TiO_2 \overset{(((}{\rightarrow} TiO_2\left(e^- + h^+\right) \quad (8)$$

$$O_2 + e^- \rightarrow O_2^-\cdot \quad (9)$$

$$O_2^-\cdot + 2H^+ \rightarrow HO_2\cdot \quad (10)$$

$$h^+ + H_2O \rightarrow H^+ + \cdot OH \quad (11)$$

Besides the sonoluminescence, ultrasound can inhibit the recombination of electron–hole pairs, extend the lifetime of carrier charge, induce particle disaggregation, and finally promote the penetration of light in wastewater. Table 2 summarizes the system, reaction conditions, and effects of typical ultrasound and photocatalytic oxidation treatment methods for degrading organic wastewater. Bembibre et al. [48] reported that approximately 57.0% and 94.0% of tetracycline were completely mineralized in 180 min in the ultrasound field and photocatalysis process (λ = 400–750 nm), respectively, whereas 100% of tetracycline was mineralized in 90 min in the combination of ultrasound with the photocatalysis process (Table 2; No. 3). In this system, ultrasound power plays a significant role. Excessive ultrasound power can generate excessive cavitation bubbles, making them unable to collapse in positive and negative pressure cycles, forming many ineffective bubbles, reducing energy transfer speed, and forming an ultrasound barrier.

$O_3$ is usually added in the combination system of ultrasound with a photocatalytic oxidation process, and UV can enhance the decomposition of $O_3$ to produce ·OH, which degrades organics together with the ·OH generated by ultrasound (Equations (12) and (13)). In such a system, the importance of the flow rate of $O_3$, power of UV, and ultrasound account for 40.0%, 30.0%, and 30.0%, respectively [50]. The combination of ultrasound–light with other treatment methods is commonly used to treat pharmaceutical wastewater, such as amoxicillin, sulfadiazine, and dye wastewater, such as direct orange 26 and toluidine blue.

$$O_3 + H_2O + UV \rightarrow H_2O_2 + O_2 \quad (12)$$

$$H_2O_2 + UV \rightarrow \cdot OH \quad (13)$$

The frequency range in the ultrasound photocatalytic oxidation process is approximately 20–55 kHz. However, Giannakis et al. used a higher frequency (275 kHz) ultrasound to treat *E. coli* in the ultrasound-UV-FE process, proving that high-frequency ultrasound can damage the cell membrane, making the bacteria more susceptible to attack [51].

**Table 2.** Typical applications of ultrasound-assisted photocatalytic oxidation process in organic wastewater treatment.

| No. | Study System | Pollutants | Ultrasound | | Experimental Conditions | Removal Efficiency | Ref. |
|---|---|---|---|---|---|---|---|
| | | | Power (W) | Frequency (kHz) | | | |
| 1 | Ultrasound–visible light–N–$TiO_2$ | Amoxicillin | - | 20 | pH = 5.8, N-$TiO_2$ = 0.5 g $L^{-1}$, amoxicillin = 10 mg $L^{-1}$ | 37.0% | [52] |
| 2 | Ultrasound–visible light–F–$TiO_2$ | Crystal violet | 285 | 44–55 | pH = 7.0, reaction time = 120 min, F-$TiO_2$ = 0.1 g/L | >80.0% | [53] |
| 3 | Ultrasound–visible light–Ca–ZnO | Tetracycline | 100 | 40 | LED = 1.6 W, Ca-ZnO = 0.5 g/L | 99.0% | [48] |
| 4 | Ultrasound–UV–$TiO_2$ | Phenol | 50 | 24 | UV = 11 W, $TiO_2$ = 0.1 g $L^{-1}$ | - | [54] |
| 5 | Ultrasound–UV–MCs | Sulfadiazine | 200 | - | pH = 11.0, reaction time = 150 min, UV = 150 W, MCs = 0.9 g $L^{-1}$ | 100%<br>TOC = 89.0%<br>COD = 96.0% | [55] |
| 7 | Ultrasound–UV–$O_3$ | Atrazine | 142.5 | - | UV = 75 W, $O_3$ = 10.75 g $h^{-1}$ | 97.7% | [50] |
| 8 | Ultrasound–UV–PS | Trichloroethylene | 95 | 24 | pH = 5.5, reaction time = 20 min, PS = 61 μmol $L^{-1}$, trichloroethylene = 61 μmol $L^{-1}$ | 96.3% | [56] |
| 9 | Ultrasound–UV–PMS | Direct orange 26 | 125 | 20 | pH = 7.0, PMS = 1.5 mmol $L^{-1}$ | 100% | [57] |
| 10 | Ultrasound–UV–PMS–MNPs@C | BPA | 200 | 20 | pH = 6.0, UV-C lamp = 6 W, mechanical stirrer = 200 r $min^{-1}$, T = 25 ± 1 °C | 100% | [58] |
| 11 | Ultrasound–UV–FE | *E. coli* | 20 | 275 | pH = 4.5–5.0, ferrozine solution = 4.9 mmol $L^{-1}$, hydroxylamine hydrochloride solution = 10.0% (*w*/*w*) | 100% | [51] |
| 12 | | Toluidine blue | 70 | - | pH = 4.0, PVP/$Fe_3O_4$@$SiO_2$ = 0.07 g, $H_2O_2$ = 1.0 mol $L^{-1}$, toluidine blue = 4 × $10^{-4}$ mol/L | 95.3% | [59] |
| 13 | | 17 emerging pollutants | - | 375 | pH = 7.48, $Fe^{2+}$ = 5 mg $L^{-1}$, oxalic acid = 2 mg $L^{-1}$, power density = 88 W $L^{-1}$ | - | [60] |

#### 3.2.3. Combination of Ultrasound Field with MW Field

In the system of the combination of ultrasound filed with MW filed, ultrasound and MW are often treated separately, which determines that wastewater can only be treated by ultrasound and MW alone. Therefore, how to simultaneously perform ultrasound–MW processing is an interesting research direction. When using the system to degrade phenol, the ·OH produced by the cavitation of ultrasound is the primary oxidant; the MW field is used to increase the rotational migration and friction of polar molecules, thereby increasing the collisions between reactants, and considerably reducing the reaction time. The order of the degradation rate constant is that ultrasound–MW > MW > ultrasound, which shows that the system has strong synergy, and the enhancement effect of MW is higher than that of ultrasound degradation. Wu et al. [61] reported that the degradation of phenol by ultrasound and MW produced better results (65.0%) than that of ultrasound or MW alone (35.0%).

### *3.3. Ultrasound-Enhanced Organic Wastewater Treatment Methods*

#### 3.3.1. Ultrasound–Heterogeneous Fenton-like System

Ultrasound and heterogeneous Fenton-like processes are typical physical and chemical treatment methods of organic wastewater, respectively. They can work alone and work together to mutually promote their capacity, i.e., like adding glass balls, heterogeneous FE catalysts can provide cavitation nuclei for cavitation bubbles [62]. However, excessive loading may cause the weakening of the treatment efficiency of organic wastewater due to the scavenging of ·OH using an excessive catalytic element [62].

There are multiple transition metal elements that can initiate the Fenton-like catalytic process, including Fe, Cu, Mn, and Pb [63,64], while Fe-based catalysts and Cu-based catalysts are common ones. Fe-based Fenton-like catalysts consist of synthetic catalysts such as $MnFe_2O_4$/biochar, Fe-Mo/rGo [15], Fe/Cu@γ-$Al_2O_3$ [16], and Fe/Acid-montmorillonite [65], iron ores, solid waste such as coal fly ash, slag, and gangue [6,66–69], and zero-valent iron. Table 3 summarizes the system, reaction conditions, and effects of typical ultrasound and FE methods for degrading organic wastewater. The essence of Fe-based catalysts is the electron transfer between ≡Fe (III) and ≡Fe (II), i.e., ≡Fe (III), as the electron acceptor, can accept an electron to generate ≡Fe (II) that can initiate a Fenton-like reaction (Equations (14) and (15)). Other transition metal elements (Cu, Mn, Pb, etc.) show a similar catalytic mechanism.

$$\equiv Fe^{III} + H_2O_2 \rightarrow \equiv Fe(OOH)^{II} + H^+ \quad (14)$$

$$\equiv Fe(OOH)^{II} \overset{(((}{\rightarrow} \equiv Fe^{II} + HO_2\cdot \quad (15)$$

where the symbol ≡represents the iron species bound to the surface of the catalyst.

It has been confirmed by many studies that the presence of ultrasound can significantly enhance the performance of heterogeneous Fenton-like processes. Bremner et al. [67] found that a silent Fenton-like reaction can only remove 10.0% TOC in 6 h in the treatment of phenol, while the value increased to 29.0% in the ultrasound–Fenton-like process. Panda et al. [70] reported that only 25.0% of decabromodiphenyl ether can be removed by a Fenton-like process alone, while the addition of ultrasound can raise the removal rate to 92.0% in 60 min and achieve 100% removal in 80 min. In addition, the presence of ultrasound can widen the optimal pH range as well, i.e., from 3.0 to approximately 2.0–5.0, which may decrease the dosage of acid or base in the adjustment of pH. The ultrasound–FE system shows a good performance in degrading various wastewater, such as industrial textile wastewater, olive will wastewater, dye wastewater, and pharmaceutical wastewater. The frequency range of the ultrasound-FE process is between 20 and 50 kHz. Bremner et al. [67] believe that high-frequency ultrasound generated by disc transducers can more effectively generate free radicals and prolong the efficiency of oxidation reactions compared to low-frequency ultrasound.

**Table 3.** Typical applications of ultrasound-assisted FE process in organic wastewater treatment.

| No. | Study System | Pollutants | Ultrasound | | Experimental Conditions | Removal Efficiency | Ref. |
|---|---|---|---|---|---|---|---|
| | | | Power (W) | Frequency (kHz) | | | |
| 1 | Ultrasound–FE–$Fe^{2+}$ | Emerging contaminants | - | 400 | $Fe^{2+}$ = 0.5 mmol $L^{-1}$, SDZ = 0.1 mmol $L^{-1}$ | - | [68] |
| 2 | | Acid scarlet | - | - | pH = 4.5, $Fe^{2+}$ = 0.045 mmol $L^{-1}$, $H_2O_2$ = 66 mmol $L^{-1}$, GR = 300 mg $L^{-1}$, GR: $H_2O_2$: $Fe^{2+}$ = 100:15:41 | 96.6% | [66] |
| 3 | | C.I. reactive yellow 145 | 80 | 35 | pH = 3.0, reaction time = 60 min, $Fe^{2+}$ = 20 mg $L^{-1}$, $H_2O_2$ = 20 mg $L^{-1}$ | 95.0% COD = 51.0% | [71] |
| 4 | | Reactive blue 19 | 100 | 53 | pH = 3.67, $Fe^{2+}$ = 48.98 mg $L^{-1}$, $H_2O_2$ = 300 mg $L^{-1}$ | 85.0% | [72] |
| 5 | | Carbofuran | - | 40 | pH = 3.0, reaction time = 120 min, $Fe^{2+}$ = 20 mg $L^{-1}$, $H_2O_2$ = 100 mg $L^{-1}$, initial carbofuran = 20 mg $L^{-1}$ | 99.0% mineralisation = 46.0% | [73] |
| 6 | | Textile wastewater | 120 | 40 | pH = 3.0, reaction time = 60 min, $Fe^{2+}$ = 0.05 g $L^{-1}$, $H_2O_2$ = 1 g $L^{-1}$ | 97.5% | [74] |
| 7 | | Olive mill wastewater | 100 | 20 | pH = 3.5, $H_2O_2$/Fe = 1.5, $H_2O_2$/COD = 0.73 | TPH = 80.0% .toxicity = 13.0-17.0% COD = 26.0% | [69] |
| 8 | | Ciprofloxacin | - | 580 | pH = 3.0, $H_2O_2$ = 14.2 mmol $L^{-1}$, $H_2O_2/Fe^{2+}$ = 6, T = 30 ± 1 °C | mineralisation rate = 60.0%. | [75] |
| 9 | | Industrial textile wastewater | - | 35 | pH = 3.0, reaction time = 60 min, $Fe^{2+}$ = 0.05 g $L^{-1}$, $H_2O_2$ = 1.65 g $L^{-1}$ | 99.0% | [76] |
| 10 | Ultrasound–FE–nZVI | Decabromodiphenyl ether | - | 20 | pH = 2.0, $Fe^{2+}$ = 0.5 g $L^{-1}$, $H_2O_2$ = 150 mg $L^{-1}$ | TOC = 60.0% | [70] |
| 11 | | Azo dyes | - | - | pH = 2.0, reaction time = 60 min, $H_2O_2$ = 20 mg $L^{-1}$, $Fe^{2+}$ = 1 g $L^{-1}$, dye: $H_2O_2$:$Fe^{2+}$ = 1:3.6:2.4 | 99.9% COD = 63.4% | [77] |
| 12 | Ultrasound–FE–magnetite nanoparticles | Acid blue15 | 1200 | 50 | pH = 3.0, magnetite nanoparticles = 1 g $L^{-1}$, $H_2O_2$ = 10 mmol $L^{-1}$ | 99.3% TOC = 40.4% | [29] |
| 13 | Ultrasound–FE–sponge iron | Chloramphenicol | 200 | 20 | pH = 3.0, $Fe^{2+}$ = 2.26 g $L^{-1}$, $H_2O_2$ = 3.19 mmol $L^{-1}$ | 99.97% | [78] |
| 14 | Ultrasound–FE–$MnFe_2O_4$/BC | MB | 665 | 40 | pH = 5.0, reaction time = 20 min, $MnFe_2O_4$/BC = 0.7 g $L^{-1}$, $H_2O_2$ = 15 mmol $L^{-1}$, MB = 20 mg $L^{-1}$ | 100% | [62] |
| 15 | Ultrasound–FE–$Fe_2O_3$/SBA-15 | Phenol | - | 584 | $H_2O_2$ = 0.6 g $L^{-1}$ | TOC = 30.0% | [67] |
| 16 | Ultrasound-nZVI-activated carbon | [AMIM]Cl [BMBIM]Br[BMBIM]Br | - | 45 | pH = 3.0, zero-valent iron = 3 g $L^{-1}$, activated carbon = 6 g $L^{-1}$ | [AMIM]Cl = 92.9% [BMBIM]Br = 96.1% | [79] |
| 17 | Ultrasound–chitosan-stabilized nZVI | Aid fuchsine | - | 45 | pH = 4.96, chitosan-stabilized nZVI = 100 mg $L^{-1}$, reaction time = 15 min, Acid fuchsine = 0.4 g $L^{-1}$, T = 30 °C | 99.0% | [80] |
| 18 | Ultrasound–nZVI–PMS | 4-Chlorophenol | 200 | - | pH = 3.0, nZVI = 0.4 g $L^{-1}$, PMS = 1.25 mmol $L^{-1}$ | 95.0% | [81] |
| 19 | Ultrasound–FE–waste antivirus Cu film | BPA | 96.57 | 37 | pH = 5.0, $H_2O_2$ = 100 mmol $L^{-1}$, mechanical stirrer = 250 r $min^{-1}$, TA = 0.5 mmol $L^{-1}$, NaOH = 2 mmol $L^{-1}$, T = 60 °C | 100% | [82] |
| 20 | Ultrasound–FE–Cu–$C_3N_4$ | MB | 150 | 40 | pH = 6.7, reaction time = 30 min, Cu-$C_3N_4$ = 0.4 g $L^{-1}$, $H_2O_2$ = 20 mmol $L^{-1}$ | 96.0% | [83] |

3.3.2. Ultrasound–PS Oxidation System

Ultrasound can directly activate PS or indirectly oxidize PS to produce $SO_4^{-\cdot}$ through a cavitation effect ($E_0$ = 2.60 V) (Equations (16) and (17)) [84,85].

$$S_2O_8^{2-} \xrightarrow{(((} 2SO_4^{-\cdot} \quad (16)$$

$$S_2O_8^{2-} + \cdot OH \rightarrow HSO_4^- + SO_4^{-\cdot} + \frac{1}{2}O_2 \quad (17)$$

As shown in Figure 2, it can be seen that ultrasound can increase the refresh rate of the surface of zero-valent iron by its mechanical effect and accelerate the release of $Fe^{2+}$, which can react with PS to generate $SO_4^{-\cdot}$, i.e., the existence of zero-valent iron adds a path of the indirect generation of $SO_4^{-\cdot}$ [86]. Similarly, the Fe element existing in other forms such as $Fe_3O_4$ and scrap iron can play a similar role.

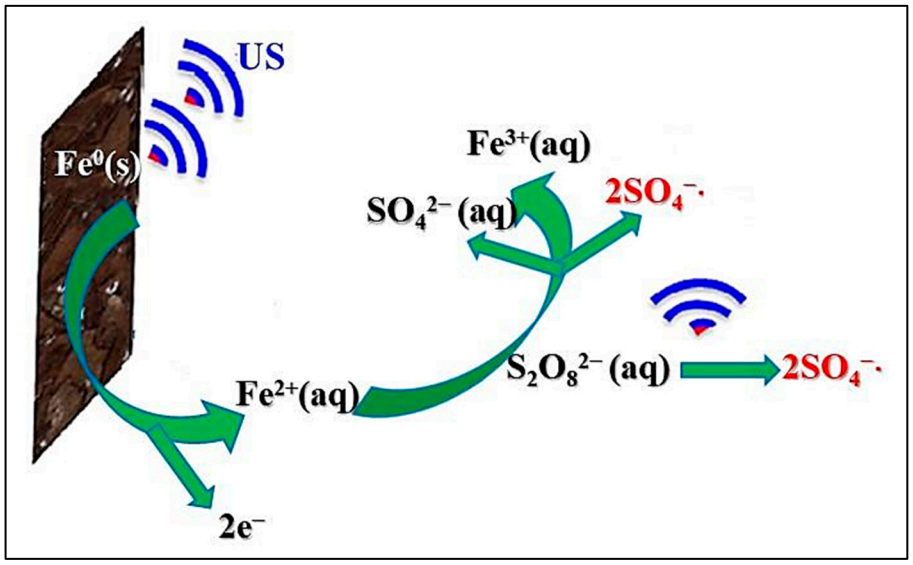



**Figure 2.** Working mechanism of ultrasound–PS–zero–valent iron process [86].

The ultrasound−PS oxidation system is effective in the oxidative degradation of organic pollutants, while $SO_4^{-\cdot}$ could play a primary role compared with ·OH. Malakotian et al. [87] reported that the removal rate of tetracycline decreased from 92.6% to 84.0% and 27.4%, respectively, in the presence of tert-butyl alcohol (·OH scavenger) and methanol ($SO_4^{-\cdot}$ radical scavenger), indicating that the majority of tetracycline was oxidized by $SO_4^{-\cdot}$ [87].

3.3.3. Ultrasound-Membrane System

Recently, ultrasound has been widely applied in membrane fouling control, relying on its mechanical effect and chemical effect on the surface of the fouled membrane because the mechanical effect can increase the flow speed of solute and form an eddy on the membrane surface that can cause physical damage and dispersion of the filter cake layer, while the ·OH generated by the chemical effect of ultrasound can chemically degrade the dirt layer on the membrane surface.

Research has shown that the presence of ultrasound can significantly reduce trans-membrane pressure, thereby reducing membrane fouling [88,89]. However, in recent years, researchers have found that using dual-frequency and triple-frequency ultrasound can form a more uniform standing wave field to better reduce membrane fouling, while the stable wave field generated by single-frequency ultrasound can lead to the uneven distribution of ultrasound, which can easily lead to membrane damage [90]. Therefore, compared to single-frequency ultrasound, dual-frequency and triple-frequency ultrasound are more effective in controlling membrane fouling.

What we should notice is that membrane damage may be caused when the mechanical effect and chemical effect of ultrasound directly act on the bare membrane. Thus, retaining a certain filter cake layer and reducing the power and working time of ultrasound are necessary to avoid this phenomenon. Wen et al. [91] reported that membrane damage can be effective avoided when the ultrasound power was 0.12 W $cm^{-2}$ and worked for 5 min every 60 min in the process of the filtration of anaerobic-activated sludge.

Activated carbon is an effective technology to eliminate trace organic matter. Adding it to the membrane filtration system can improve the permeation quality. The results of the separate study of activated carbon under the action of ultrasound on emerging pollutants show that the presence of ultrasound enhances the adsorption capacity and kinetic rate constant, and the combination of acoustic flow with cavitation increases the dynamic rate and the increase in proximity to equilibrium. Secondes et al. [92] reported that the removal rate of pollutants was less than 10.0% when the membrane was treated alone, and it increased to 99.0% when activated carbon and ultrasound (35 kHz) were added [92].

### *3.4. Ultrasound–Physical Fields–Chemical Treatment Methods*

#### 3.4.1. Ultrasound–EC–PS Process

As mentioned in Section 3.3.2, $SO_4^{-}\cdot$ can be generated under the action of ultrasound; however, this process is also accompanied by the production of $SO_4^{2-}$ (Equation (18)). Subsequently, the researchers found that the addition of an electric field can anodize $SO_4^{2-}$ to PS (Equation (19)), which forms a cyclic reaction. Moreover, due to the degassing effect caused by ultrasound, more $SO_4^{2-}$ can be adsorbed and converted to $S_2O_8^{2-}$ at the anode (Equation (19)) [4]. According to the report of Yousefi et al. [32], in the presence of ultrasound (130 kHz), the removal rate of COD increased from 69.0 to 91.2% (Table 1; No. 8). The kinetic study showed that the remove of COD from petrochemical wastewater via the ultrasound–EC–PS process accorded with the pseudo-second-order reaction, and the regression coefficient is 0.89 [32].

$$S_2O_8^{2-} \overset{(((}{\rightarrow} SO_4^{-}\cdot + SO_4^{2-} \quad (18)$$

$$SO_4^{2-} \rightarrow S_2O_8^{2-} + e^- \quad (19)$$

#### 3.4.2. Ultrasound–EC–FE Process

When $O_2$ is supplied through the aeration device, $H_2O_2$ is produced on the cathode via the EC method and then converted into ·OH on the anode to degrade organic pollutants (Equations (20) and (21)). Although the sound flow generated by ultrasound may lead to degassing, ultrasound can increase the production of $H_2O_2$ via electrolysis by improving mass transfer, and the degassing effect of ultrasound is not significant at normal reaction temperatures (30 °C, 25%) [93]. Additionally, $Fe^{3+}$ can be quickly reduced to $Fe^{2+}$ at the cathode, thereby forming a circular reaction (Equation (22)) [34]. By using this process, the overall damage of 2,4-dichlorophenoxyacetic acid (2,4-D) can be achieved in 75 min, and the addition of ultrasound increased the apparent rate constant of the reaction from 0.025 to 0.046 $min^{-1}$ in the study of Souza et al. [43] (Table 1; No. 4). Li et al. [3] reported that the decolorization rate of red X-GRL was increased from 74.9 to 86.4% with the addition of ultrasound (Table 1; No 10).

$$O_2 + 2H^+ + 2e^- \rightarrow H_2O_2 \quad (20)$$

$$Fe^{2+} + H_2O_2 + H^+ \overset{(((}{\rightarrow} Fe^{3+} + H_2O + \cdot OH \quad (21)$$

$$Fe^{3+} + e^- \rightarrow Fe^{2+} \quad (22)$$

3.4.3. Ultrasound–UV–FE Process

In the ultrasound–UV–FE process, many photons in the photo-Fenton-like process can promote the decomposition of $H_2O_2$ and the conversion of $Fe^{3+}$ to $Fe^{2+}$ in the catalyst, while ultrasound can reduce the particle size of heterogeneous catalyst and increases more available active sites. Particle size analysis indicates that the catalyst particle size in the presence of ultrasound is 0.2–10 μm, which is much smaller than the catalyst size (2 to 200 μm) in the absence of ultrasound. Segura et al. [67] used different systems to degrade phenolic wastewater. The degradation rates of pollutants in the ultrasound alone, UV alone, UV–ultrasound, and ultrasound–UV treatment systems was 27.0, 37.0, 52.0, and 90.0% in 6 h, respectively, indicating that ultrasound can promote the removal of pollutant in the photo-FE process and has a strong synergistic effect with UV.

3.4.4. Ultrasound–UV–PS/PMS Process

The simultaneous application of ultrasound and UV can generate more $SO_4^{-\cdot}$ by activating PS than that in the application of ultrasound or UV alone (Equation (23)). The increase in the degradation rate constant of pollutants caused by the increase in ultrasound power is attributed to the improvement in the number of ·OH produced by cavitation and further produce the $SO_4^{-\cdot}$, while it also related to the quantum yield, which can accelerate the generation of reactive oxygen species, and thus accelerate the degradation of pollutants [56]. The degradation of trichloroethylene via the ultrasound–UV process showed a higher rate constant, which was $8.59 \times 10^{-2}$, $2.32 \times 10^{-2}$, and $2.95 \times 10^{-2}$ $min^{-1}$, respectively, compared with treatment by a single UV or ultrasound, indicating that the combined process had a higher synergistic effect (synergy index 1.62), and the results in the final removal rate of trichloroethylene reached 100% (Equation (24)). Nonetheless, in the corresponding treatment in the presence of PS, the removal rates of trichloroethylene by UV and ultrasound were only 41.2% and 51.8%, respectively (Table 2; No. 9) [56].

$$S_2O_8^{2-} \xrightarrow{UV} 2SO_4^{-}\cdot \quad (23)$$

$$\text{Synergy index} = \frac{k_{(\text{ultrasound+UV+PS})}}{k_{(\text{ultrasound+PS})} + k_{(\text{UV+PS})}} \quad (24)$$

In addition to PS, ultrasound and UV can cleave the O-O bond in PMS ($E_0$ = 1.81 V) to produce $SO_4^{-}\cdot$ [57]. The addition of ultrasound and UV broadens the range of pH (3.0–9.0) of organic wastewater treatment. The addition of ultrasound can accelerate the conversion of $Fe^{3+}$ to $Fe^{2+}$, thereby reducing the pH sensitivity of the system and expanding the pH range. In the system, R = 1.22, which indicates that the system has strong synergy, and the comprehensive system effect exceeds the sum of the individual processes [58] (Table 2; No. 11).

*3.5. Advantages and Disadvantages of Ultrasound in the Treatment of Organic Wastewater*

The advantages and disadvantages of the ultrasound treatment of organic wastewater are listed in Table 4. Ultrasound technology has the advantages of no secondary pollution. In addition, ultrasound can accelerate the reaction rate and decrease the dosage of chemicals and wastewater treatment cost when ultrasound is used to enhance other wastewater treatment methods. However, ultrasound treatment of wastewater alone is not economical. When ultrasound is combined with other treatment methods, the commonly used power range is 20–665 W. As the power increases, the number of ultrasound cavitation bubbles will also increase, which means that the cavitation effect will be enhanced, but high power also means high energy consumption [27]. In Oturan et al.'s study, adding 20 W ultrasound to the EC-FE process can shorten the time for the complete mineralization of pollutants from 100 min to 75 min [34]. This is because the addition of ultrasound increases mass transfer, rapidly reducing oxygen to $H_2O_2$ at the cathode, thereby increasing the rate of ·OH production, while when the power is greater than 20 W, the degassing effect caused

by ultrasound is more significant, leading to a decrease in dissolved oxygen in the solution, and then the amount of $H_2O_2$ produced at the cathode decreases. Therefore, we can reduce the energy consumption of the treatment method and improve the efficiency of wastewater treatment by combining low-power ultrasound with other treatment methods.

**Table 4.** Advantages and disadvantages of ultrasound in the treatment of organic wastewater.

| Advantages | Disadvantages |
| --- | --- |
| No secondary pollution;<br>Accelerate the reaction rate;<br>Reducing dosage of chemicals;<br>Reducing wastewater treatment cost by combining with other wastewater treatment methods. | Consuming electrical energy;<br>Making noise. |

## 4. Typical Ultrasound-Enhanced Organic Wastewater Treatment Equipment

### *4.1. Classification by Reactor Type*

#### 4.1.1. Ultrasound Cleaning Tank-Type Reactor

Ultrasound cleaning tank-type reactors are usually equipped with transducers on both sides (No. 7 in Figure 3a) or at the bottom of the reactor (No. 4 in Figure 3b). The advantage of the installation position of the transducer is that the transducer can be controlled easily to adjust the output power, and corrosion of the transducer can be avoided [94].

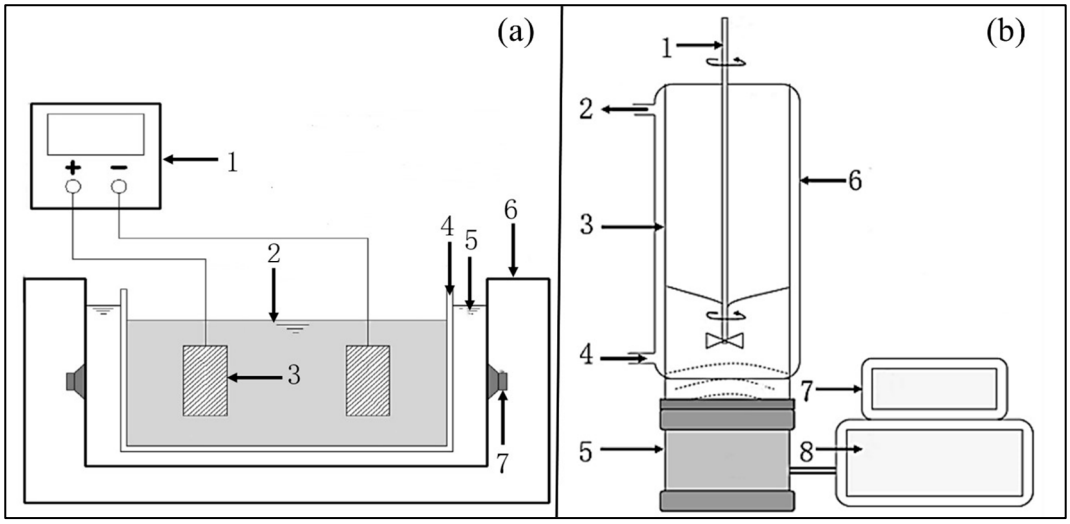



**Figure 3.** Device diagram of (**a**) ultrasound cleaning tank reactor and (**b**) ultrasound amplifier coupled transducer [4,67]. ((**a**) 1. Power supply, 2. wastewater, 3. electrode, 4. Perspex vessel, 5. water (20 °C), 6. ultrasound generation, 7. ultrasound transducer. (**b**) 1. Stirrer, 2. cooling water outlet, 3. cylindrical glass reactor, 4. cooling water inlet, 5. ultrasound transducer, 6. cooling jacket, 7. ultrasound amplifier and frequency controller, 8. ultrasound power supply).

As shown in Figure 3a, the temperature of the cooling water (No. 5) in the cleaning tank can be adjusted to control the temperature of the wastewater in Perspex vessel (No. 4) to achieve the optimal treatment temperature. In addition, researchers can achieve the optimal frequency and power of ultrasound by adjusting the transducer. Yang et al. removed more than 94.0% of COD from cephalosporin pharmaceutical wastewater by using this experimental device [4].

As shown in Figure 3b, ultrasound with a frequency of 3.82–140 kHz can be generated by a disk transducer (No. 5) at the bottom of the glass reactor (No. 3) [29]. The reactor is surrounded by a cooling jacket (No. 6) to achieve the required treatment temperature. This kind of device can easily output high-frequency ultrasound to effectively realize cavitation conditions. Bremner et al. [67] obtained a 29.0% removal rate of TOC in the aqueous phenol solutions by using the device in Figure 3b.

4.1.2. Ultrasound Probe Reactor

As shown in Figure 4, the probe transducer (No. 2) is the most important part of the reactor. The maximum transmission coefficient of ultrasound takes place along the axial direction of the probe and drops sharply in the radial direction of the probe. In addition, the emission power of the probe is adjustable. As the small diameter of the probe limits its effective working range, the use of this kind of reactor has been limited to the laboratory stage until now [71].

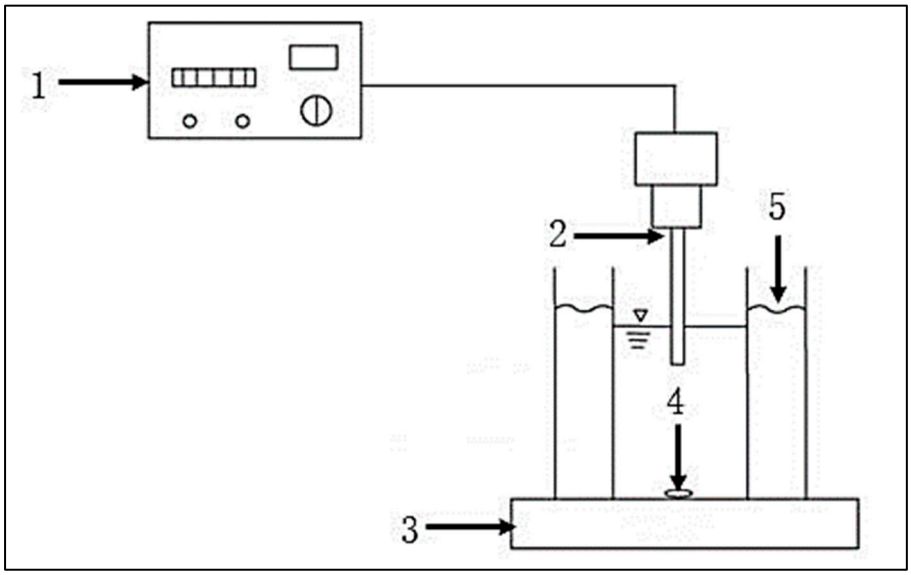



**Figure 4.** The device diagram of ultrasound probe reactor [71]. (1. Ultrasound generator reactor, 2. probe transducer, 3. magnetic stirrer, 4. magnetic bar, 5. constant temperature water bath).

It is noteworthy that this kind of reactor is convenient to use, but the probe immersed in the solution can be eroded easily using the mechanical effect of ultrasound, and the vibration from the probe will raise the temperature of the solution and affect its service life. Thus, low-temperature liquid should be circulated in the jacket when necessary [94].

The treatment efficiency of organic wastewater in such a kind of reactor cannot satisfy people's requirements. However, ultrasound can play an excellent auxiliary role and promote the efficiency of organic degradation when combined with other methods. Peng et al. [95] reported that only 4.0% of polycyclic aromatic hydrocarbons were degraded by ultrasound alone in 120 min, while the degradation rate reached 84.8% in the ultrasound-PS process. In addition, in the treatment of carbofuran [73], the removal efficiency of carbofuran (99.0%) in the ultrasound–FE process was much higher than that (60.0%) in the ultrasound alone system.

The above two types of reactors are the mainstream reactors at present, whereas the liquid whistle reactor is not common now. Unlike transducers, ultrasound in the liquid whistle reactor is generated by the jet impinging on the metal blade (No. 3, Figure 5). The sound intensity in the reactor can be adjusted by changing the shape of the jet. In addition, ultrasound frequency can be adjusted by the flow rate. This kind of reactor is always used in the emulsification and homogenization of oily wastewater [96].

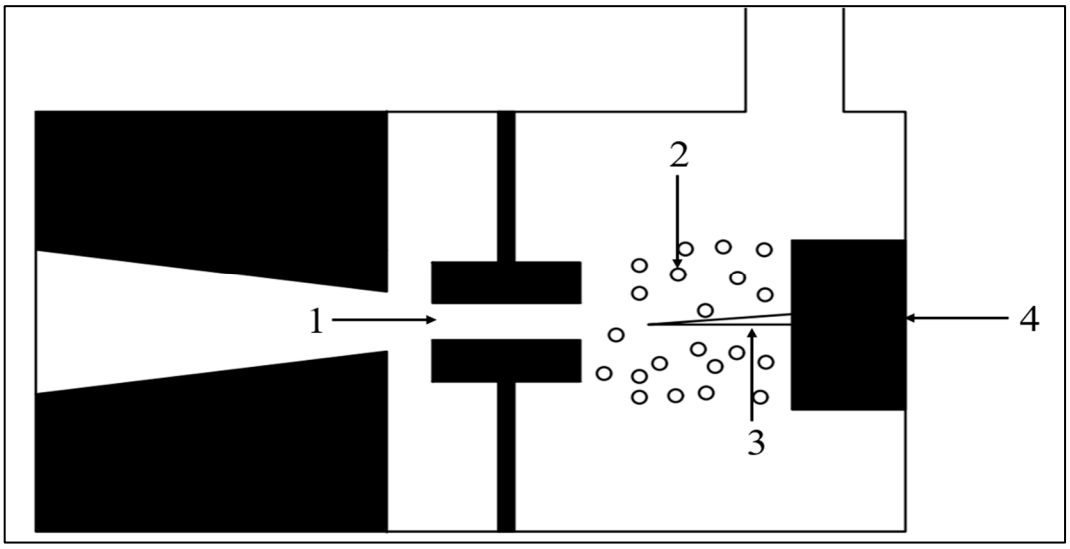



**Figure 5.** Device diagram of the liquid whistle-type ultrasound reactor [96]. (1. Adjustable channel for liquid flow, 2. cavitation zone, 3. metal blade, 4. stainless steel block).

#### 4.1.3. Comparison of Ultrasound Reactors with Different Types

Table 5 compares the advantages and disadvantages of three types of ultrasound reactors. Firstly, the cleaning tank reactor has a wide range of uses and can be used to clean experimental equipment. It is relatively common to simply place the reaction tank in the cleaning tank during the reaction, and the external water bath can also control the temperature, but this also limits the size of the reaction tank. Subsequently, the ultrasound probe-type reactor only needs to insert the probe into the reaction solution during reaction, which is easy to operate. However, the ultrasound distribution is uneven, and the probe is prone to corrosion after long-term use. Finally, liquid whistle-type reactors are uncommon now, which are used for the averaging and emulsification of oily wastewater.

**Table 5.** Comparison of different types of reactors.

| Reactors | Advantages | Disadvantages |
|---|---|---|
| Ultrasound cleaning tank-type reactor | Ultrasound wave is evenly distributed;<br>Can easily control temperature. | Limiting the reactor size. |
| Ultrasound probe reactor | Uneven distribution of ultrasound wave;<br>The probe is prone to corrosion. | Easy operation. |
| Liquid whistle reactor | Application in homogenization of oily wastewater. | Ancient, with certain limitations. |

### *4.2. Classified According to Liquid Flow Mode*

#### 4.2.1. Fully Mixed Reactor

The ultrasound cleaning tank-type reactor and ultrasound probe reactor can both work in fully mixed mode. The fully mixed reactor can be used in various ultrasound processes, including ultrasound alone, the ultrasound–PS process, the ultrasound–FE process, the ultrasound–electrochemistry process, the ultrasound–photocatalytic oxidation process, etc.

When ultrasound works alone or works with PS or a Fenton-like process, the reaction can be easily started by adding PS or $Fe^{2+}/H_2O_2$ to the system. However, in the ultrasound–electrochemistry process (Figure 6a) the addition of an anode and cathode at both sides of the reactor (No. 3 and 5) is necessary. In addition, particle electrode may be needed as well if the fully mixed reactor can play the role of a three-dimensional electrode system. When the fully mixed reactor works with the photocatalytic oxidation process, UV lamp (No. 3, Figure 6b) or other light sources and a photocatalyst are needed.

The fully mixed reactor is generally equipped with a mechanical stirrer to evenly mix the wastewater and chemical reagents [97]. If the temperature and pH need to be controlled,

a temperature controller and pH sensor will be set, respectively. The wastewater in the fully mixed reactor can be easily mixed uniformly. However, the capacity of the fully mixed reactor is limited, and it cannot work in a continuous mode. The treatment efficiency of organic wastewater in such a kind of reactor is very high, for example, the decolorization rate of reactive black 5 dye treated by the reactor, outlined in Figure 6a, reached 89.0% [45], while 99.9% rhodamine 6G and 88.7% phenol were removed by the reactor, as outlined in Figure 6b [98].

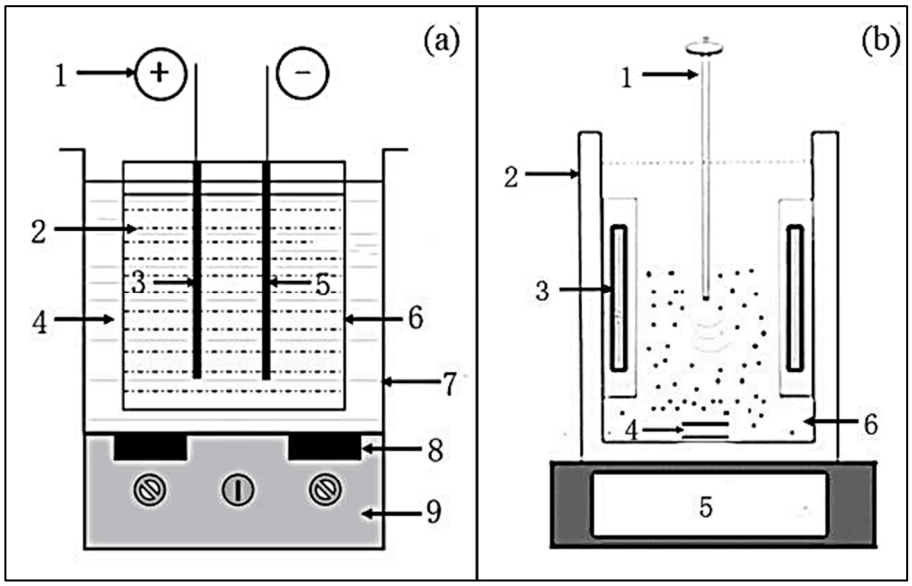



**Figure 6.** Experimental device of (**a**) ultrasound−EC process, and (**b**) continuous stirred tank of ultrasound−UV process [45,98]. ((**a**) 1. DC power supply, 2. dye solution, 3. anode, 4. distilled water, 5. cathode, 6. glass reactor, 7. ultrasound bath, 8. transducer, 9. ultrasound control unit. (**b**) 1. Ultrasound probe, 2. cooling water jacket, 3. UV lamp, 4. magnetic bar, 5. magnetic stirrer, 6. dye solution).

#### 4.2.2. Continuous Reactor

In the continuous reactor, the ultrasound unit always works with other organic wastewater treatment units, and common treatment processes include, but are not limited to, the ultrasound–$O_3$ process (Figure 7a), the ultrasound–MW process (Figure 7b), the ultrasound–membrane process (Figure 7c), etc.

As for the ultrasound–$O_3$ process, the organic wastewater is first filtered by coarse sand (No. 3) and fine sand (No. 4) and then sequentially entered into the UV unit (No. 5) and the ultrasound unit (No. 6). After the treatment, the treated organic wastewater can be discharged. Both of the bottoms of the UV unit and ultrasound unit are equipped with $O_3$ generators (No. 7). They can determine the optimal scheme to adjust the experimental scheme. Using this device, 97.7% of atrazine was degraded in the study of Jing et al. [50].

As for the ultrasound–MW process, the function of MW is to control temperature. After the ultrasound treatment (No. 6), organic wastewater enters the circulation system for cooling. A control center is usually set (No. 8) to control the flow, temperature, and MW power. Using this device, up to 76.0% of phenol was degraded in the study of Wu et al. [61], which is equivalent to the sum of the degradation achieved by the separate treatment of ultrasound and MW.

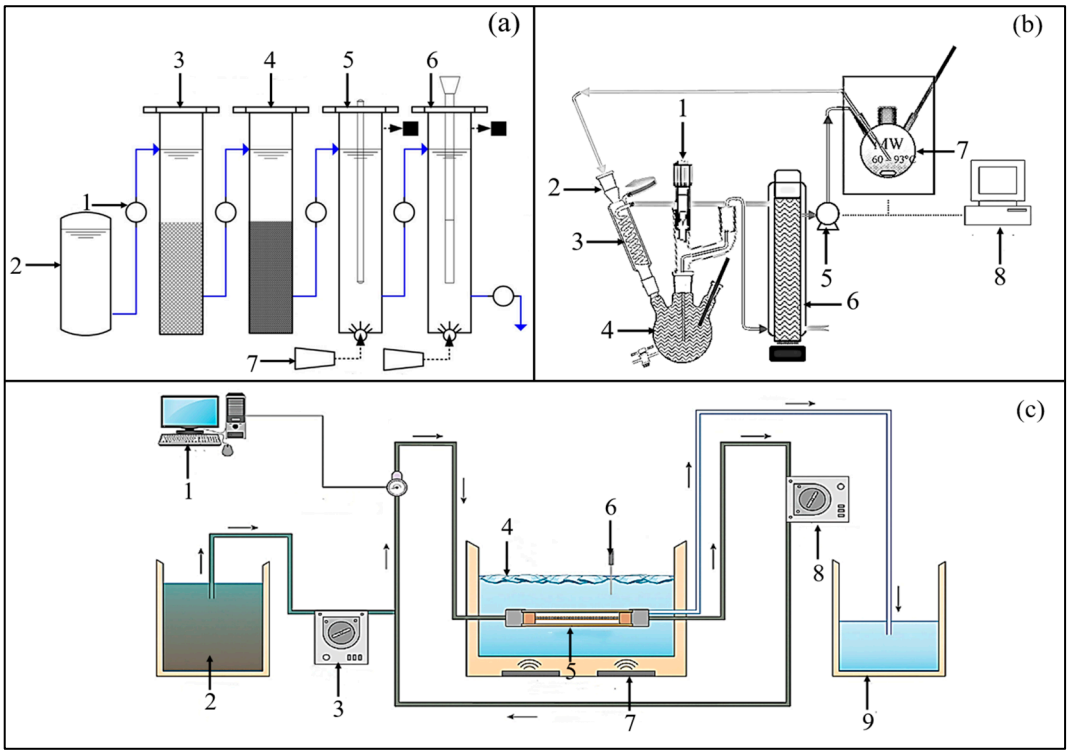



**Figure 7.** Experimental device diagram of (**a**) push flow reactor of ultrasound–UV–$O_3$ process, (**b**) ultrasound–MW process, (**c**) ultrasound-membrane process [50,61,92]. ((**a**) 1. Pump, 2. storage tank, 3. coarse sand, 4. fine sand, 5. UV unit, 6. ultrasound unit, 7. $O_3$ generators. (**b**) 1. Inlet, 2. cooling water outlet, 3. intensive condenser, 4. outlet and sampler, 5. pump, 6. ultrasound generator, 7. MW generator, 8. control center. (**c**) 1. Pressure meter and transducer, 2. feed tank, 3. peristaltic pump, 4. ice, 5. membrane module, 6. ultrasound bath, 7. temperature probe, 8. peristaltic pump, 9. permeate tank).

As for the ultrasound–membrane process, the membrane module (No. 5) is usually immersed in the ultrasound bath (No. 6), and then the wastewater is pumped into the ultrasound bath and flows out after the ultrasound treatment and membrane filtration. The continuous reactor is suitable for the tandem treatment of wastewater by sequentially passing the treatment units. The disadvantage is that the reactor design is complex, and the operation cost is high.

#### 4.2.3. Comparison of Ultrasound Reactors with Different Flow Modes

Table 6 is a comparative table of advantages and disadvantages classified by flow mode. For a fully mixed flow reactor, the reaction solution can be completely mixed and fully reacted, and the operation is simple, but it can only be reacted in batches. For continuous flow reactors, the solution can be continuously treated, but different types of treatment methods require redesigning the reactor, which is costly.

**Table 6.** Comparison of reactors with different flow modes.

| Types | Advantages | Disadvantages |
|---|---|---|
| Fully mixed reactor | Mix the solution evenly. Convenient combination with other processing methods. | Unable to process continuously. |
| Continuous reactor | Continuous processing. | Complex design and high cost. |

## 5. Development Prospect of Ultrasound in the Treatment of Organic Wastewater

It is well know that economic cost is a critical impediment for the use of ultrasound in industrial applications [24]. However, the operating cost can be controlled by optimizing the operating conditions. For example, ultrasound treatment can reduce the required battery voltage. In addition, it can increase the pH of the reaction and enlarge the range of organic wastewater treatment. Novel attempts for cost reduction are urgently required to increase the scope of this method. Several suggestions about knowledge gaps and research requirements are discussed below.

(1) Deeply investigate the advantages and disadvantages of the coupling of ultrasound with other treatment methods in order to provide a reference of the potential novel coupling of ultrasound with other organic wastewater treatment methods.
(2) Explore new work modes of ultrasound, for example, dual-frequency mode or triple-frequency mode, in order to achieve a possible reduction in energy consumption.
(3) Apply numerical simulation to optimize the ultrasound reactor structure by enhancing the cavitation effect, for example, Monte Carlo simulation can assist artificial neural networks to determine the contribution of three effects of ultrasound (mechanical effect, chemical effect, and thermal effect).
(4) Explore new operation methods to enhance the cavitation effect, such as adding solid particles and increasing mechanical stirring, thus improving the effectiveness of ultrasound.

## 6. Conclusions

Our review presented different aspects of ultrasound waves in the treatment of organic wastewater. The cavitation effect of ultrasound has huge potential in the application of organic wastewater treatments, making the combination of ultrasound with other organic wastewater treatment methods exhibit strong synergistic effects, i.e., compensate their own shortcomings and enhance the degradation efficiency of organic wastewater. The following conclusions can be drawn.

(1) When combined with other methods, the mechanical effect of ultrasound can clean the surface of solid material and enhance mass transfer, while the chemical effect and thermal effect of ultrasound can generate ·OH and PS to promote the reaction rate and thus accelerate the degradation of organic pollutants.
(2) Ultrasound can increase the removal rate of TN and TP by promoting the growth of algae. In addition to that, ultrasound can control membrane pollution, thereby enabling the effective filtration of pollutants by the membrane.
(3) In ultrasound waves, PS and PMS can generate more oxidizing free radicals to degrade organic pollutants. Additionally, ultrasound can activate nZVI to generate the FE reaction to degrade pollutants.
(4) According to the different reactor types, the ultrasound reactors can be divided into two types: ultrasound cleaning tank-type reactors and ultrasound probe reactors. The ultrasound generated by the ultrasound cleaning tank reactor is more uniform, while the probe-type reactor is more convenient. In addition, there is a liquid whistle reactor, in which ultrasound is generated by a mechanical effect. According to the liquid circulation mode, the ultrasound reactors can be divided into two types as well, in which the fully mixed type is applicable to almost all reactions of the ultrasound–enhanced organic wastewater treatment, while the continuous reactor can achieve the sequential processing of ultrasound and other processing methods of organic wastewater treatment.

**Author Contributions:** Resources, conceptualization, writing—review and editing, funding acquisition, visualization, N.W. and X.B.; writing—original draft, data curation, investigation, L.L.; investigation, K.W. and X.H.; writing—review and editing, supervision, Y.H. and X.M.; data curation, investigation, M.W. and X.L. All authors have read and agreed to the published version of the manuscript.

**Funding:** This research was funded by [the National Natural Science Foundation of China] grant number [51808039], [Zhiyuan Science Foundation of BIPT] grant number [2023013], and [the National College Students Innovation and Entrepreneurship Training Program] grant numbers [2023J00007; 2022J00024].

**Institutional Review Board Statement:** Not applicable.

**Informed Consent Statement:** Not applicable.

**Data Availability Statement:** The data that support the findings of this study are available from the corresponding author upon reasonable request.

**Conflicts of Interest:** The authors declare that there is no conflict of interest.

## Nomenclature

| Variable | Description |
|---|---|
| Ultraviolet | UV |
| Electrochemical | EC |
| Persulphate | PS |
| Microwave | MW |
| bonded high valent Fe | ≡Fe (III) |
| bonded low valent Fe | ≡Fe (II) |
| Nano zero valent iron | nZVI |
| Peroxymonosulphate | PMS |
| Bisphenol A | MPA |
| Methylene Blue | MB |

## References

1. Babu, S.G.; Ashokkumar, M.; Neppolian, B. The Role of Ultrasound on Advanced Oxidation Processes. *Top Curr. Chem.* **2016**, *374*, 75. [CrossRef]
2. Zhang, Q.-Q.; Jin, R.-C. The Application of Low-Intensity Ultrasound Irradiation in Biological Wastewater Treatment: A Review. *Crit. Rev. Environ. Sci. Technol.* **2015**, *45*, 2728–2761. [CrossRef]
3. Li, H.; Lei, H.; Yu, Q.; Li, Z.; Feng, X.; Yang, B. Effect of low frequency ultrasonic irradiation on the sonoelectro-Fenton degradation of cationic red X-GRL. *Chem. Eng. J.* **2010**, *160*, 417–422. [CrossRef]
4. Yang, B.; Zuo, J.; Li, P.; Wang, K.; Yu, X.; Zhang, M. Effective ultrasound electrochemical degradation of biological toxicity and refractory cephalosporin pharmaceutical wastewater. *Chem. Eng. J.* **2016**, *287*, 30–37. [CrossRef]
5. Rasheed, Q.J.; Pandian, K.; Muthukumar, K. Treatment of petroleum refinery wastewater by ultrasound-dispersed nanoscale zero-valent iron particles. *Ultrason. Sonochem.* **2011**, *18*, 1138–1142. [CrossRef] [PubMed]
6. Abdelhay, A.; Othman, A.A.; Albsoul, A. Treatment of slaughterhouse wastewater using high-frequency ultrasound: Optimization of operating conditions by RSM. *Environ. Technol.* **2021**, *42*, 4170–4178. [CrossRef] [PubMed]
7. Liu, W.; Huang, F.; Liao, Y.; Zhang, J.; Ren, G.; Zhuang, Z.; Zhen, J.; Lin, Z.; Wang, C. Treatment of $Cr^{VI}$-Containing $Mg(OH)_2$ Nanowaste. *Angew. Chem.* **2008**, *120*, 5701–5704. [CrossRef]
8. Dong, Y.; Yuan, H.; Ge, D.; Zhu, N. A novel conditioning approach for amelioration of sludge dewaterability using activated carbon strengthening electrochemical oxidation and realized mechanism. *Water Res.* **2022**, *220*, 118704. [CrossRef]
9. Chang, T.; Wang, Y.; Wang, Y.Q.; Zhao, Z.; Shen, Z.; Huang, Y.; Veerapandian, S.K.P.; De Geyter, N.; Wang, C.; Chen, Q.; et al. A critical review on plasma-catalytic removal of VOCs: Catalyst development, process parameters and synergetic reaction mechanism. *Sci. Total Environ.* **2022**, *828*, 154290. [CrossRef]
10. Feng, X.; Wang, B.; Gao, G.; Gao, S.; Xie, C.; Shi, J.-W. $Mn_yCo_{3-y}O_x$ bimetallic oxide prepared by ultrasonic technology for significantly improved catalytic performance in the reduction of $NO_x$ with $NH_3$. *Fuel* **2023**, *352*, 129159. [CrossRef]
11. Chen, D.; Wang, Q.; Li, Y.; Li, Y.; Zhou, H.; Fan, Y. A general linear free energy relationship for predicting partition coefficients of neutral organic compounds. *Chemosphere* **2020**, *247*, 125869. [CrossRef] [PubMed]
12. Suna, S.; Liu, H.; Zhang, J.; Wang, W.; Xu, P.; Zhu, X.; Wang, Y.; Wan, S. Application of a novel coagulant in reservoir water treatment in Qingdao. *Desalin. Water Treat.* **2023**, *284*, 49–60. [CrossRef]
13. Yaqub, A.; Ajab, H. Applications of sonoelectrochemistry in wastewater treatment system. *Rev. Chem. Eng.* **2013**, *29*, 123–130. [CrossRef]
14. Scannapieco, D.; Naddeo, V.; Belgiorno, V. Control of fouling in MBRs through nanospheres addition. *Desalin. Water Treat.* **2014**, *55*, 702–711. [CrossRef]
15. Qin, W.; Ma, Y.; He, T.; Hu, J.; Gao, P.; Yang, S. Enhanced Heterogeneous Fenton-like Process for Sulfamethazine Removal via Dual-Reaction-Center Fe-Mo/rGO Catalyst. *Nanomaterials* **2022**, *12*, 4138. [CrossRef]

16. Zhu, G.F.; Xiong, S.H.; Shi, C.; Jin, Y.; Ge, M.Q. Ceria-promoted heterogeneous Fenton-like oxidation of polyvinyl alcohol, Rhodamine-B, and Reactive Red X-3B over Fe/Cu@gamma-$Al_2O_3$ microspheres under neutral conditions. *J. Alloys Compd.* **2022**, *924*, 15. [CrossRef]
17. Musielak, G.; Mierzwa, D.; Kroehnke, J. Food drying enhancement by ultrasound—A review. *Trends Food Sci. Technol.* **2016**, *56*, 126–141. [CrossRef]
18. Yu, Q.; Fan, L.; Li, J. A novel process for asparagus polyphenols utilization by ultrasound assisted adsorption and desorption using resins. *Ultrason. Sonochem.* **2020**, *63*, 104920. [CrossRef]
19. Liao, T.; Xi, Y.; Zhang, L.; Li, J.; Cui, K. Removal of toxic arsenic (As()) from industrial wastewater by ultrasonic enhanced zero-valent lead combined with $CuSO_4$. *J. Hazard. Mater.* **2021**, *408*, 124464. [CrossRef]
20. Cardenas Sierra, R.S.; Zuniga-Benitez, H.; Penuela, G.A. Elimination of cephalexin and doxycycline under low frequency ultrasound. *Ultrason. Sonochem.* **2021**, *79*, 105777. [CrossRef]
21. Pirsaheb, M.; Moradi, N. A systematic review of the sonophotocatalytic process for the decolorization of dyes in aqueous solution: Synergistic mechanisms, degradation pathways, and process optimization. *J. Water Process Eng.* **2021**, *44*, 102314. [CrossRef]
22. Ritesh, P.; Srivastava, V.C. Understanding of ultrasound enhanced electrochemical oxidation of persistent organic pollutants. *J. Water Proc. Eng.* **2020**, *37*, 101378. [CrossRef]
23. Zhu, Y.; Fan, W.; Feng, W.; Wang, Y.; Liu, S.; Dong, Z.; Li, X. A critical review on metal complexes removal from water using methods based on Fenton-like reactions: Analysis and comparison of methods and mechanisms. *J. Hazard. Mater.* **2021**, *414*, 125517. [CrossRef]
24. Yang, L.; Xue, J.; He, L.; Wu, L.; Ma, Y.; Chen, H.; Li, H.; Peng, P.; Zhang, Z. Review on ultrasound assisted persulfate degradation of organic contaminants in wastewater: Influences, mechanisms and prospective. *Chem. Eng. J.* **2019**, *378*, 122146. [CrossRef]
25. Wang, L.; Luo, D.; Hamdaoui, O.; Vasseghian, Y.; Momotko, M.; Boczkaj, G.; Kyzas, G.Z.; Wang, C. Bibliometric analysis and literature review of ultrasound-assisted degradation of organic pollutants. *Sci. Total Environ.* **2023**, *876*, 162551. [CrossRef]
26. Hassani, A.; Malhotra, M.; Karim, A.V.; Krishnan, S.; Nidheesh, P.V. Recent progress on ultrasound-assisted electrochemical processes: A review on mechanism, reactor strategies, and applications for wastewater treatment. *Environ. Res.* **2022**, *205*, 112463. [CrossRef]
27. de Andrade, F.V.; Augusti, R.; de Lima, G.M. Ultrasound for the remediation of contaminated waters with persistent organic pollutants: A short review. *Ultrason. Sonochem.* **2021**, *78*, 105719. [CrossRef] [PubMed]
28. Arefi-Oskoui, S.; Khataee, A.; Safarpour, M.; Orooji, Y.; Vatanpour, V. A review on the applications of ultrasonic technology in membrane bioreactors. *Ultrason. Sonochem.* **2019**, *58*, 104633. [CrossRef]
29. Prakash, L.V.; Gopinath, A.; Gandhimathi, R.; Velmathi, S.; Ramesh, S.T.; Nidheesh, P.V. Ultrasound aided heterogeneous Fenton degradation of Acid Blue 15 over green synthesized magnetite nanoparticles. *Sep. Purif. Technol.* **2021**, *266*, 118230. [CrossRef]
30. Luo, X.; Gong, H.; He, Z.; Zhang, P.; He, L. Recent advances in applications of power ultrasound for petroleum industry. *Ultrason. Sonochem.* **2021**, *70*, 105337. [CrossRef]
31. Yang, B.; Zuo, J.; Tang, X.; Liu, F.; Yu, X.; Tang, X.; Jiang, H.; Gan, L. Effective ultrasound electrochemical degradation of methylene blue wastewater using a nanocoated electrode. *Ultrason. Sonochem.* **2014**, *21*, 1310–1317. [CrossRef]
32. Yousefi, N.; Pourfadakari, S.; Esmaeili, S.; Babaei, A.A. Mineralization of high saline petrochemical wastewater using Sonoelectro-activated persulfate: Degradation mechanisms and reaction kinetics. *Microchem. J.* **2019**, *147*, 1075–1082. [CrossRef]
33. Heredia-Rivera, U.; Ferrer, I.; Vazquez, E. Ultrasonic Molding Technology: Recent Advances and Potential Applications in the Medical Industry. *Polymers* **2019**, *11*, 667. [CrossRef]
34. Oturan, M.A.; Sirés, I.; Oturan, N.; Pérocheau, S.; Laborde, J.-L.; Trévin, S. Sonoelectro-Fenton process: A novel hybrid technique for the destruction of organic pollutants in water. *J. Electroanal. Chem.* **2008**, *624*, 329–332. [CrossRef]
35. Chen, X.; Bayanheshig; Jiao, Q.; Tan, X.; Wang, W. Numerical simulation of ultrasonic enhancement by acoustic streaming and thermal effect on mass transfer through a new computation model. *Int. J. Heat Mass Transfer* **2021**, *171*, 121074. [CrossRef]
36. Zhang, M.; Zhang, Z.; Liu, S.; Peng, Y.; Chen, J.; Yoo Ki, S. Ultrasound-assisted electrochemical treatment for phenolic wastewater. *Ultrason. Sonochem.* **2020**, *65*, 105058. [CrossRef]
37. Serna-Galvis, E.A.; Silva-Agredo, J.; Giraldo-Aguirre, A.L.; Florez-Acosta, O.A.; Torres-Palma, R.A. High frequency ultrasound as a selective advanced oxidation process to remove penicillinic antibiotics and eliminate its antimicrobial activity from water. *Ultrason. Sonochem.* **2016**, *31*, 276–283. [CrossRef] [PubMed]
38. Panda, D.; Sethu, V.; Manickam, S. Kinetics and mechanism of low-frequency ultrasound driven elimination of trace level aqueous perfluorooctanesulfonic acid and perfluorooctanoic acid. *Chem. Eng. Process.—Process Intensif.* **2019**, *142*, 107542. [CrossRef]
39. Matouq, M.; Al-Ayed, O.; Al-Anber, Z.; Al-Shannag, M.; Kloub, N.; Tagawa, T.; Aljbour, S. Wastewater Treatment Resulting from an Oil Shale Retorting at High Frequency Ultrasound Waves with a Chemical Elemental Analysis. *Energy Sources Part A Recovery Util. Environ. Eff.* **2010**, *32*, 1878–1884. [CrossRef]
40. Ren, H.-Y.; Zhu, J.-N.; Kong, F.; Xing, D.; Zhao, L.; Ma, J.; Ren, N.-Q.; Liu, B.-F. Ultrasonic enhanced simultaneous algal lipid production and nutrients removal from non-sterile domestic wastewater. *Energy Convers. Manag.* **2019**, *180*, 680–688. [CrossRef]
41. Chang, J.-H.; Ellis, A.V.; Yan, C.-T.; Tung, C.-H. The electrochemical phenomena and kinetics of EDTA–copper wastewater reclamation by electrodeposition and ultrasound. *Sep. Purif. Technol.* **2009**, *68*, 216–221. [CrossRef]

42. Radi, M.A.; Nasirizadeh, N.; Mirjalili, M.; Rohani Moghadam, M. Ultrasound-assisted electrochemical decolorization of anthraquinone dye C.I Reactive Blue 49, its optimization and synergic effect: A comparative study. *Int. J. Environ. Sci. Technol.* **2018**, *16*, 2455–2464. [CrossRef]
43. Souza, F.L.; Saéz, C.; Lanza, M.R.V.; Cañizares, P.; Rodrigo, M.A. Removal of herbicide 2,4-D using conductive-diamond sono-electrochemical oxidation. *Sep. Purif. Technol.* **2015**, *149*, 24–30. [CrossRef]
44. Dionisio, D.; Motheo, A.J.; Sáez, C.; Canizares, P.; Rodrigo, M.A. Coupling Ultrasound to the Electro-Oxidation of Methyl Paraben Synthetic Wastewater: Effect of Frequency and Supporting Electrolyte. *ChemElectroChem* **2018**, *6*, 1199–1205. [CrossRef]
45. Johin, J.; Nidheesh, P.V.; Sivasankar, T. Sono-electro-chemical Treatment of Reactive Black 5 Dye and Real Textile Effluent Using $MnSO_4/Na_2S_2O_8$ Electrolytes. *Arabian J. Sci. Eng.* **2019**, *44*, 9987–9996. [CrossRef]
46. Darvishi Cheshmeh Soltani, R.; Jorfi, S.; Alavi, S.; Astereki, P.; Momeni, F. Electrocoagulation of textile wastewater in the presence of electro-synthesized magnetite nanoparticles: Simultaneous peroxi- and ultrasonic-electrocoagulation. *Sep. Sci. Technol.* **2019**, *55*, 945–954. [CrossRef]
47. Cai, Y.; Li, J.; Qu, G.; Ren, N.; Zou, H.; Hu, Y.; Qiu, W. Research on dynamics and mechanism of treatment on phenol simulated wastewater by the ultrasound cooperated electro-assisted micro-electrolysis. *Water Environ. Res.* **2021**, *93*, 1243–1253. [CrossRef]
48. Bembibre, A.; Benamara, M.; Hjiri, M.; Gómez, E.; Alamri, H.R.; Dhahri, R.; Serrà, A. Visible-light driven sonophotocatalytic removal of tetracycline using Ca-doped ZnO nanoparticles. *Chem. Eng. J.* **2022**, *427*, 132006. [CrossRef]
49. Zheng, Y.; Liu, Y.; Guo, X.; Chen, Z.; Zhang, W.; Wang, Y.; Tang, X.; Zhang, Y.; Zhao, Y. Sulfur-doped g-$C_3N_4$/rGO porous nanosheets for highly efficient photocatalytic degradation of refractory contaminants. *J. Mater. Sci. Technol.* **2020**, *41*, 117–126. [CrossRef]
50. Jing, L.; Chen, B.; Wen, D.; Zheng, J.; Zhang, B. Pilot-scale treatment of atrazine production wastewater by UV/$O_3$/ultrasound: Factor effects and system optimization. *J. Environ. Manag.* **2017**, *203*, 182–190. [CrossRef]
51. Giannakis, S.; Papoutsakis, S.; Darakas, E.; Escalas-Canellas, A.; Petrier, C.; Pulgarin, C. Ultrasound enhancement of near-neutral photo-Fenton for effective E. coli inactivation in wastewater. *Ultrason. Sonochem.* **2015**, *22*, 515–526. [CrossRef] [PubMed]
52. Karim, A.V.; Shriwastav, A. Degradation of amoxicillin with sono, photo, and sonophotocatalytic oxidation under low-frequency ultrasound and visible light. *Environ. Res.* **2021**, *200*, 111515. [CrossRef] [PubMed]
53. Panahian, Y.; Arsalani, N.; Nasiri, R. Enhanced photo and sono-photo degradation of crystal violet dye in aqueous solution by 3D flower like F-$TiO_2$(B)/fullerene under visible light. *J. Photochem. Photobiol. A* **2018**, *365*, 45–51. [CrossRef]
54. Van de Moortel, W.; Kamali, M.; Sniegowski, K.; Braeken, L.; Degrève, J.; Luyten, J.; Dewil, R. How Photocatalyst Dosage and Ultrasound Application Influence the Photocatalytic Degradation Rate of Phenol in Water: Elucidating the Mechanisms Behind. *Water* **2020**, *12*, 1672. [CrossRef]
55. Hayati, F.; Isari, A.A.; Anvaripour, B.; Fattahi, M.; Kakavandi, B. Ultrasound-assisted photocatalytic degradation of sulfadiazine using MgO@CNT heterojunction composite: Effective factors, pathway and biodegradability studies. *Chem. Eng. J.* **2020**, *381*, 122636. [CrossRef]
56. Bahrami, H.; Eslami, A.; Nabizadeh, R.; Mohseni-Bandpi, A.; Asadi, A.; Sillanpää, M. Degradation of trichloroethylene by sonophotolytic-activated persulfate processes: Optimization using response surface methodology. *J. Clean. Prod.* **2018**, *198*, 1210–1218. [CrossRef]
57. Ahmadi, M.; Ghanbari, F. Combination of UVC-LEDs and ultrasound for peroxymonosulfate activation to degrade synthetic dye: Influence of promotional and inhibitory agents and application for real wastewater. *Environ. Sci. Pollut. Res. Int.* **2018**, *25*, 6003–6014. [CrossRef] [PubMed]
58. Takdastan, A.; Kakavandi, B.; Azizi, M.; Golshan, M. Efficient activation of peroxymonosulfate by using ferroferric oxide supported on carbon/UV/US system: A new approach into catalytic degradation of bisphenol A. *Chem. Eng. J.* **2018**, *331*, 729–743. [CrossRef]
59. Ghobashy, M.M.; Elbarbary, A.M.; Hegazy, D.E. Synthesis of poly (vinylpyrrolidone)/$Fe_3O_4$@$SiO_2$ nanoporous catalyst by γ-rays and evaluation their sono-photo-Fenton degradation of toluidine blue under magnetic field. *Appl. Organomet. Chem.* **2021**, *35*, e6388. [CrossRef]
60. Serna-Galvis, E.A.; Botero-Coy, A.M.; Martinez-Pachon, D.; Moncayo-Lasso, A.; Ibanez, M.; Hernandez, F.; Torres-Palma, R.A. Degradation of seventeen contaminants of emerging concern in municipal wastewater effluents by sonochemical advanced oxidation processes. *Water Res.* **2019**, *154*, 349–360. [CrossRef] [PubMed]
61. Wu, Z.L.; Ondruschka, B.; Cravotto, G. Degradation of Phenol under Combined Irradiation of Microwaves and Ultrasound. *Environ. Sci. Technol.* **2008**, *42*, 8083–8087. [CrossRef] [PubMed]
62. Cheng, Z.; Luo, S.; Li, X.; Zhang, S.; Thang Nguyen, T.; Guo, M.; Gao, X. Ultrasound-assisted heterogeneous Fenton-like process for methylene blue removal using magnetic $MnFe_2O_4$/biochar nanocomposite. *Appl. Surf. Sci.* **2021**, *566*, 150654. [CrossRef]
63. Liu, H.; Xu, T.; Li, C.; Liu, W.; Lichtfouse, E. High increase in biodegradability of coking wastewater enhanced by Mn ore tailings in Fenton/$O_3$ combined processes. *Int. J. Environ. Sci. Technol.* **2020**, *18*, 173–184. [CrossRef]
64. Li, J.; Pham, A.N.; Dai, R.; Wang, Z.; Waite, T.D. Recent advances in Cu-Fenton systems for the treatment of industrial wastewaters: Role of Cu complexes and Cu composites. *J. Hazard. Mater.* **2020**, *392*, 122261. [CrossRef]
65. Zhao, Y.-H.; Cai, Y.-F.; Zhang, Q.-J.; Wang, H.; Liu, Y.-L. Fe/Acid-montmorillonite as effective Fenton-like catalyst for the removal of methylene blue. *J. Chem. Technol. Biotechnol.* **2022**, *97*, 3163–3171. [CrossRef]

66. Liu, T.; He, F.W.; Zhang, Y.Q. Synergistic Degradation of Acid Scarlet Dyeing Wastewater by the Ultrasound/Fenton Method. *Appl. Mech. Mater.* **2013**, *448–453*, 34–37. [CrossRef]
67. Bremner, D.H.; Molina, R.; Martínez, F.; Melero, J.A.; Segura, Y. Degradation of phenolic aqueous solutions by high frequency sono-Fenton systems (US–$Fe_2O_3$/SBA-15–$H_2O_2$). *Appl. Catal. B* **2009**, *90*, 380–388. [CrossRef]
68. Xu, L.; Zhang, X.; Han, J.; Gong, H.; Meng, L.; Mei, X.; Sun, Y.; Qi, L.; Gan, L. Degradation of emerging contaminants by sono-Fenton process with in situ generated $H_2O_2$ and the improvement by P25-mediated visible light irradiation. *J. Hazard. Mater.* **2020**, *391*, 122229. [CrossRef]
69. Ciggin, A.S.; Sarica, E.S.; Doğruel, S.; Orhon, D. Impact of ultrasonic pretreatment on Fenton-based oxidation of olive mill wastewater—Towards a sustainable treatment scheme. *J. Clean. Prod.* **2021**, *313*, 127948. [CrossRef]
70. Panda, D.; Manickam, S. Heterogeneous Sono-Fenton treatment of decabromodiphenyl ether (BDE-209): Debromination mechanism and transformation pathways. *Sep. Purif. Technol.* **2019**, *209*, 914–920. [CrossRef]
71. Zhang, H.; Fu, H.; Zhang, D. Degradation of C.I. Acid Orange 7 by ultrasound enhanced heterogeneous Fenton-like process. *J. Hazard. Mater.* **2009**, *172*, 654–660. [CrossRef]
72. Siddique, M.; Farooq, R.; Price, G.J. Synergistic effects of combining ultrasound with the Fenton process in the degradation of Reactive Blue 19. *Ultrason. Sonochem.* **2014**, *21*, 1206–1212. [CrossRef] [PubMed]
73. Ma, Y.S.; Sung, C.F.; Lin, J.G. Degradation of carbofuran in aqueous solution by ultrasound and Fenton processes: Effect of system parameters and kinetic study. *J. Hazard. Mater.* **2010**, *178*, 320–325. [CrossRef]
74. Asghar, A.; Ramzan, N.; Jamal, B.U.; Maqsood, M.; Sajjadi, B.; Chen, W.Y. Low frequency ultrasonic-assisted Fenton oxidation of textile wastewater: Process optimization and electrical energy evaluation. *Water Environ. J.* **2019**, *34*, 523–535. [CrossRef]
75. Gonzalez Labrada, K.; Alcorta Cuello, D.R.; Saborit Sanchez, I.; Garcia Batle, M.; Manero, M.H.; Barthe, L.; Jauregui-Haza, U.J. Optimization of ciprofloxacin degradation in wastewater by homogeneous sono-Fenton process at high frequency. *J. Environ. Sci. Health A Tox Hazard Subst. Environ. Eng.* **2018**, *53*, 1139–1148. [CrossRef] [PubMed]
76. Cetinkaya, S.G.; Morcali, M.H.; Akarsu, S.; Ziba, C.A.; Dolaz, M. Comparison of classic Fenton with ultrasound Fenton processes on industrial textile wastewater. *Sustain. Environ. Res.* **2018**, *28*, 165–170. [CrossRef]
77. Basturk, E.; Alver, A. Modeling azo dye removal by sono-fenton processes using response surface methodology and artificial neural network approaches. *J. Environ. Manag.* **2019**, *248*, 109300. [CrossRef] [PubMed]
78. Meng, X.; Liu, Z.; Wang, S.; Kong, F. Synergistic Degradation of Chloramphenicol by an Ultrasound-Enhanced Fenton-like Sponge Iron System. *Water* **2021**, *13*, 3561. [CrossRef]
79. Zhou, H.; Lv, P.; Qi, H.; Ma, J.; Wang, J. Removal of residual functionalized ionic liquids from water by ultrasound-assisted zero-valent iron/activated carbon. *Environ. Technol.* **2019**, *40*, 2504–2512. [CrossRef]
80. Jin, X.; Zhuang, Z.; Yu, B.; Chen, Z.; Chen, Z. Functional chitosan-stabilized nanoscale zero-valent iron used to remove acid fuchsine with the assistance of ultrasound. *Carbohydr. Polym.* **2016**, *136*, 1085–1090. [CrossRef]
81. Barzegar, G.; Jorfi, S.; Zarezade, V.; Khatebasreh, M.; Mehdipour, F.; Ghanbari, F. 4-Chlorophenol degradation using ultrasound/peroxymonosulfate/nanoscale zero valent iron: Reusability, identification of degradation intermediates and potential application for real wastewater. *Chemosphere* **2018**, *201*, 370–379. [CrossRef] [PubMed]
82. Chu, J.H.; Kang, J.K.; Park, S.J.; Lee, C.G. Bisphenol A degradation using waste antivirus copper film with enhanced sono-Fenton-like catalytic oxidation. *Chemosphere* **2021**, *276*, 130218. [CrossRef]
83. Wang, C.; Huang, R.; Sun, R.; Wang, H. Ultrasound assisted Fenton-like degradation of dyes using copper doped graphitic carbon nitride. *Water Sci. Technol.* **2021**, *84*, 1146–1158. [CrossRef] [PubMed]
84. Movahedian Attar, H.; Darvishmotevalli, M.; Moradnia, M. Degradation of 4-chlorophenol from aqueous solution using ultrasound/persulphate: Prediction by RSM. *Int. J. Environ. Anal. Chem.* **2020**, *102*, 6030–6040. [CrossRef]
85. Moradnia, M.; Noorisepehr, M.; Salari, M.; Darvishmotevalli, M. Optimization of 2-Chlorophenol Removal Using Ultrasound/Persulfate: Prediction by RSM Method, Biodegradability Improvement of Petrochemical Refinery Wastewater. *Arabian J. Sci. Eng.* **2021**, *47*, 6931–6939. [CrossRef]
86. Weng, C.H.; Tsai, K.L. Ultrasound and heat enhanced persulfate oxidation activated with Fe(0) aggregate for the decolorization of C.I. Direct Red 23. *Ultrason. Sonochem.* **2016**, *29*, 11–18. [CrossRef] [PubMed]
87. Malakotian, M.; Asadzadeh, S.N.; Khatami, M.; Ahmadian, M.; Heidari, M.R.; Karimi, P.; Firouzeh, N.; Varma, R.S. Protocol encompassing ultrasound/$Fe_3O_4$ nanoparticles/persulfate for the removal of tetracycline antibiotics from aqueous environments. *Clean Technol. Environ. Policy* **2019**, *21*, 1665–1674. [CrossRef]
88. Li, D.J.; Li, M.; Wang, Y.; Gong, C.P. Optimization of the operating parameters for online ultrasonic on controlling membrane fouling in SMBR. *Desalin. Water Treat.* **2013**, *51*, 3832–3839. [CrossRef]
89. Wang, Z.; Chen, C.; Liu, H.; Hrynshpan, D.; Savitskaya, T.; Chen, J.; Chen, J. Enhanced denitrification performance of Alcaligenes sp. TB by Pd stimulating to produce membrane adaptation mechanism coupled with nanoscale zero-valent iron. *Sci. Total Environ.* **2020**, *708*, 135068. [CrossRef]
90. Lin, X.; Lu, K.; Hardison, A.K.; Liu, Z.; Xu, X.; Gao, D.; Gong, J.; Gardner, W.S. Membrane inlet mass spectrometry method (REOX/MIMS) to measure 15N-nitrate in isotope-enrichment experiments. *Ecol. Indic.* **2021**, *126*, 107639. [CrossRef]
91. Wen, X.; Sui, P.; Huang, X. Exerting ultrasound to control the membrane fouling in filtration of anaerobic activated sludge--mechanism and membrane damage. *Water Sci. Technol.* **2008**, *57*, 773–779. [CrossRef] [PubMed]

92. Secondes, M.F.; Naddeo, V.; Belgiorno, V.; Ballesteros, F., Jr. Removal of emerging contaminants by simultaneous application of membrane ultrafiltration, activated carbon adsorption, and ultrasound irradiation. *J. Hazard. Mater.* **2014**, *264*, 342–349. [CrossRef]
93. Chen, W.S.; Huang, C.P. Decomposition of nitrotoluenes in wastewater by sonoelectrochemical and sonoelectro-Fenton oxidation. *Ultrason. Sonochem.* **2014**, *21*, 840–845. [CrossRef]
94. Meroni, D.; Djellabi, R.; Ashokkumar, M.; Bianchi, C.L.; Boffito, D.C. Sonoprocessing: From Concepts to Large-Scale Reactors. *Chem. Rev.* **2022**, *122*, 3219–3258. [CrossRef] [PubMed]
95. Peng, L.; Wang, L.; Hu, X.; Wu, P.; Wang, X.; Huang, C.; Wang, X.; Deng, D. Ultrasound assisted, thermally activated persulfate oxidation of coal tar DNAPLs. *J. Hazard. Mater.* **2016**, *318*, 497–506. [CrossRef] [PubMed]
96. Mason, T.J.; Paniwnyk, L.; Lorimer, J.P. The uses of ultrasound in food technology. *Ultrason. Sonochem.* **1996**, *3*, S253–S260. [CrossRef]
97. Ghanbari, F.; Zirrahi, F.; Lin, K.-Y.A.; Kakavandi, B.; Hassani, A. Enhanced electro-peroxone using ultrasound irradiation for the degradation of organic compounds: A comparative study. *J. Environ. Chem. Eng.* **2020**, *8*, 104167. [CrossRef]
98. Demir, N.; Gunduz, G.; Dukkanci, M. Degradation of a textile dye, Rhodamine 6G (Rh6G), by heterogeneous sonophotoFenton process in the presence of Fe-containing $TiO_2$ catalysts. *Environ. Sci. Pollut. Res. Int.* **2015**, *22*, 3193–3201. [CrossRef]

**Disclaimer/Publisher's Note:** The statements, opinions and data contained in all publications are solely those of the individual author(s) and contributor(s) and not of MDPI and/or the editor(s). MDPI and/or the editor(s) disclaim responsibility for any injury to people or property resulting from any ideas, methods, instructions or products referred to in the content.